This is to certify that the

thesis entitled

IMPLEMENTATION AND TESTING OF A
LASER INDUCED FLUORESCENCE SYSTEM FOR THE
CHARACTERIZATION OF A MULTIPOLAR
ELECTRON CYCLOTRON RESONANCE PLASMA REACTOR

presented by

GREGORY LOUIS KING

has been accepted towards fulfillment
of the requirements for

Master of Science degree in Electrical Engineering

Timothy Grotjohn

Major professor

Date August 9, 1991

IMPLEMENTATION AND TESTING OF A LASER INDUCED FLUORESCENCE SYSTEM FOR THE CHARACTERIZATION OF A MULTIPOLAR ELECTRON CYCLOTRON RESONANCE PLASMA REACTOR

by

Gregory Louis King

A THESIS

Submitted to
Michigan State University
in partial fulfillment of the requirements
for the degree of

MASTER OF SCIENCE

Department of Electrical Engineering

1991

ABSTRACT

IMPLEMENTATION AND TESTING OF A
LASER INDUCED FLUORESCENCE SYSTEM FOR THE
CHARACTERIZATION OF A MULTIPOLAR
ELECTRON CYCLOTRON RESONANCE PLASMA REACTOR

by

Gregory Louis King

In materials processing using electron cyclotron resonance (ECR) plasmas the ion energy distribution is important in determining the processing rate and magnitude of any material damage. This thesis describes the concepts and implementation of the laser induced fluorescence technique as a non-intrusive measure of these distributions at various spatial locations and under various experimental conditions in a multipolar electron cyclotron resonance plasma.

This thesis begins with a discussion of the theoretical basis of laser induced fluorescence spectroscopy and its applicability to ion energy and ion density studies in an ECR plasma. With this background the ion energy within the source and processing regions of the plasma reactor is measured. Measured Doppler shifted energy distributions indicate plasma potential variation from the source to the processing region. Finally, relative metastable ion density measurements are described at various locations within the source and processing regions of the plasma reactor.

ACKNOWLEDGEMENTS

I would like to thank Dr. Timothy Grotjohn for his generosity. He has given his knowledge, his time and his support to guide me through the work presented here. I would also like to thank Dr. Jes Asmussen for his insights and advice and Dr. Donnie K. Reinhard for his comments and suggestions. Since this thesis would not have been possible without the laser accessible baseplate, I would like to thank Peng-Un Mak for his work designing this integral piece of equipment. Finally, I would like to thank Jim Bradeen for his encouragement when it was needed most and to my family for a lifetime of support.

TABLE OF CONTENTS

Chapter 3
LIF Apparatus/Multipolar ECR Plasma System

Chapter 4
Ion Energies and Velocities

Chapter 5
Relative Ion Densities

Chapter 6
Summary of Results

LIST OF TABLES

LIST OF FIGURES

Chapter 1
Introduction

1.1 Motivation for an MPDR ECR Plasma Ion Study

The scope of microwave electron cyclotron resonance (ECR) processing is increasing dramatically. Applications for the high density, low species energy, clean processor are numerous. ECR plasmas are used for etching, thin film deposition and growth of oxide layers [1-3]. For any of these the energy and density of species impinging on the processing surface is important in determining the rate of processing and the magnitude of any surface damage.

To understand the processing mechanisms, an understanding of the species dynamics is necessary. The charged particles having energy greater than the thermal energy are particularly energetic and worthy of study. Although the ion energies have been studied in a microwave plasma disk reactor (MPDR) using a multi-grid ion energy analyzer, limitations precluded a complete characterization [4].

1.2 LIF Research Goals

This thesis endeavors to describe a laser induced fluorescence system for the characterization of an MPDR ECR plasma with respect to its ion energy and density attributes. A preliminary characterization study to test and evaluate the LIF system includes a study of the ions created under various experimental parameters and at various locations. This thesis describes the method, the cautions and the preliminary results of an LIF study of singly ionized argon in an MPDR plasma.

1.3 Thesis Outline

Chapter 2 begins with a description of the theory of LIF as it relates to the measurements of later chapters. This chapter is an overview of the theory and a complete description is found in the references cited. Chapter 2 concludes with a brief look at pertinent literature using LIF as a plasma diagnostic tool.

Chapter 3 describes the MPDR source and supporting equipment. The bulk of the chapter describes the lasers, optics and light collection equipment used. Ion energy measurements are described in chapter 4. The chapter begins with a look at the various broadening mechanisms that affect the LIF absorption lineshape and continues with an ion energy measurement in the source of the MPDR. Chapter 4 concludes with a study of the ion velocity distribution in both the source and processing regions of the plasma. Chapter 5 switches to relative ion density measurements in the MPDR at various locations and under different experimental conditions. Chapter 6 summarizes the work of this thesis. An appendix is included which contains the computer program used to collect and average the LIF signal.

Chapter 2

LIF Utilized for Plasma Diagnostics: A Review

2.1 Introduction

Laser induced fluorescence (LIF) is a sensitive diagnostic tool well suited for detailed studies of ECR plasmas. The power of LIF lies in its ability to probe the plasma without intrusive probes or analyzers. Also, the spatial resolution of LIF allows detailed study of each particular region of the plasma. The following sections review the theory of absorption spectroscopy relative to the energy, velocity and density studies undertaken for this thesis.

The final section of this chapter reviews the pertinent literature in plasma diagnostics. Particular attention is paid to LIF used in ECR process plasmas under similar conditions studied in this thesis.

2.2 The Theory of Laser Induced Fluorescence

Laser induced fluorescence involves exciting an atom or ion in a ground or metastable electronic energy level to a higher energy level through absorption of laser radiation. The excited species can spontaneously decay to the beginning energy level or to another level through emission of a photon. The intensity of this emission or fluorescence is proportional to the excited state species density and indirectly proportional to the beginning state density. Also, the lineshape of the absorption radiation spectrum gives information about the energy of the excited species.

2.2.1 LIF for Ion Density Measurements

Laser induced fluorescence is particularly useful for studies of species density. The following describes the theory of LIF in terms of rate equations for transitions from one energy level to another. The fluorescence signal resulting from the emission of radiation as the ion decays from its excited state is proportional to the density (N_2 cm^{-3}) of the excited state. A relationship between the number of photons per second incident on the detector (n_p) and this density is then:

$$n_p = N_2 A_{23} \varepsilon \qquad sec^{-1} \tag{2.1}$$

where A_{23} (sec^{-1}) is the Einstein rate coefficient for spontaneous emission and ε (cm^3) is the collection coefficient based on such factors as the efficiency of the collection system and the solid angle subtended by the collection optics. The fluorescence signal is then directly proportional to the number of photons. In order to understand the relationship between this signal and the total species density, an equation for the upper level density is needed.

Finding an equation for N_2 begins with a look at a typical LIF transition, shown in Figure 2.1, where N_i is the number density of species for that level, W_{12} and W_{21} are the laser induced rates of absorption and emission, Q_{ij} is the collisional excitation or quenching rate and A_{ij} is the spontaneous emission rate [5]. Species are excited from one level to a higher one by absorption of laser radiation or collisions with other particles. Species decay to a lower energy level spontaneously, through collisions or through laser radiation induced emission.

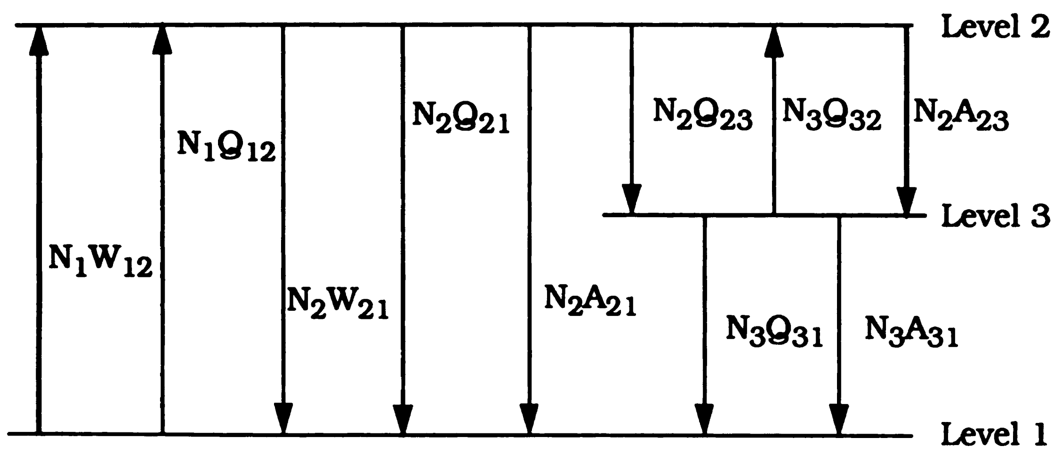

Figure 2.1: Three Level Energy Diagram

Assuming a constant total number density (N_T) for the system, the rate equations for each of the two excited levels are [6]:

$$\frac{dN_2}{dt} = N_1W_{12} - N_2(W_{21} + Q_{21} + A_{21} + Q_{23} + A_{23}) + N_3Q_{32} \tag{2.2}$$

$$\frac{dN_3}{dt} = N_2(Q_{23} + A_{23}) - N_3(Q_{31} + A_{31} + Q_{32}) \tag{2.3}$$

$$N_T = N_1 + N_2 + N_3 \tag{2.4}$$

In steady state ($dN_3/dt = 0$), the population ratio N_3/N_2 becomes:

$$\frac{N_3}{N_2} = \frac{Q_{23} + A_{23}}{Q_{31} + A_{31} + Q_{32}} = B \tag{2.5}$$

Then substituting Equation 2.4 into Equation 2.2 and assuming steady state and full saturation:

$$N_2 = \frac{W_{12}}{W_{12}(1+B)+W_{21}} N_T \tag{2.6}$$

Full saturation means the laser induced rates are larger than both spontaneous and collisional rates (W_{12}, $W_{21} >> Q_{ij}$, A_{ij}) [5].

Equation 2.6 shows that N_2 is proportional to the total species density. Earlier Equation 2.1 showed that the fluorescence signal is proportional to the level 2 number density. This leads to the conclusion that the fluorescence intensity measured is a relative measure of the total species density ($N_1 + N_2 + N_3$). Since in most systems $N_1 >> N_2$ or N_3, the LIF signal can primarily be interpreted as a measure of N_1. This conclusion is the basis for the relative density measurements of Chapter 5.

2.2.2 LIF for Ion Velocity Measurements

The Doppler effect, where the relative motion of a particle shifts the observed frequency of light emitted or absorbed by that particle, serves as the basis for the ion velocity distribution measurements using LIF. By tuning the dye laser (Section 3.3.2) through the Doppler shifted absorption wavelengths the resulting lineshape of the fluorescence intensity is proportional to the ion velocity distribution along the laser beam. In other words [7]:

$$I(\lambda)\,d\lambda = Kf(v)\,dv \tag{2.7}$$

where I is the fluorescence intensity distribution as a function of wavelength, f(v) is the velocity distribution and K is a proportionality constant. The dependence of the absorption wavelength on the ion velocity is [8]:

$$\lambda_o = \lambda\left(1 + \frac{v}{c}\right) \tag{2.8}$$

where λ is the Doppler shifted wavelength, λ_o is the center wavelength, c is the speed of light in a vacuum and v is the velocity of the ion along the laser beam. An ion with a velocity in the direction of the laser beam requires light of a shorter wavelength to make the transition to the upper energy level.

2.2.3 LIF for Ion Energy Measurements

For a Maxwellian distribution of the ion velocity at a temperature, T_i, the lineshape due to Doppler broadening has a Gaussian shape:

$$g_{dop}(\lambda - \lambda_o) = \sqrt{\frac{m_i c^2}{2\pi k T_i \lambda_o^2}} \exp\left(-\frac{m_i c^2}{2 k T_i \lambda_o^2}(\lambda - \lambda_o)\right) \tag{2.9}$$

where m_i is the mass of the ion and c is the speed of light in vacuum. The full width at half the maximum value of g (FWHM) is found from Equation 2.9 as [9]:

$$\Delta\lambda = \frac{2\lambda_o}{c}\sqrt{\frac{2kT_i \ln 2}{m_i}} \tag{2.10}$$

The ion energy or temperature is found by measuring $\Delta\lambda$ for a particular distribution and solving for T_i:

$$kT_i = \frac{m_i c^2}{8\ln 2}\left(\frac{\Delta\lambda}{\lambda_o}\right)^2 eV \tag{2.11}$$

All ion energy estimates in this work are found using this equation. The velocity distributions presented are found using Equations 2.7 and 2.8.

2.3 Recent LIF Work in Plasmas

Laser induced fluorescence has come into common usage since the advent of high powered pulsed lasers. Some of the early work in LIF plasma diagnostics is in regard to flames. Eckbreth, et al. used LIF as a density measurement in flames [10]. This work also described methods for absolute density calibration. J. W. Daily proposed operating in saturation to overcome quenching difficulties in Reference [6]. The work of Wright, et al., described the study of velocity distributions using LIF [8, 11].

Many references in the literature describe the use of LIF for density and energy measurements in a wide variety of plasmas. Various gases have been studied. Table 1.1 lists some of those gases and the energy transitions studied. Some of the species listed absorb two photons of light to make the transition to the higher energy level.

The most complete LIF studies in low pressure microwave ECR plasmas have been undertaken on diverging field ECR reactors [7, 12, 13, 14]. These plasma sources use solenoidal magnetic coils to produce the ECR fields. They are characterized by magnetic field gradients which produce associated ion drifts.

Plasma Species	Wavelength (nm) Absorption	Emission	Comment	Reference
Ar^+	611.49	460.96		12
Ar^+	617.23	458.99		15
Ar^+	624.3	488.0		16
Ar	696.54	772.4/727.3		17
CF	232.9	240.0		18
CF_2	261.7	271.0		18
Cl	210.1	904.1	Two photon	19
Cl	233.3	725-775	Three peaks in emission range	20
F	690.25	677.40		17
Ge	265.1	275.5		21
H	205.14	656.2	Two photon	22
N_2^+	389.05	389.05	Doublet emission	14
Ne	597.55	626.65		13
O	226	845	Two photon	23/24
SO	248	270/314		25
Xe	605.12	529.22		15
Zr^+	595.53	838.94		8

Table 1.1: Plasma Species Studied using LIF

Den Hartog, et al. [14] studied the energy of a nitrogen ion in an ECR discharge. They report the transverse temperature of the ion in terms of its implications in plasma etching. Their study took place in the bulk of the plasma to determine if the ion gains transverse energy before it reaches the processing surface.

A series of studies using argon and argon/helium mixtures have characterized these ECR reactors with respect to ion temperatures and ion velocity distributions [7,12,13]. These distributions were measured in both the source and processing regions of the plasma and under various experimental conditions. In an argon discharge downstream from the source with microwave power of 1.5 kWatts and at 0.35 mTorr, an ion energy upper bound of 0.46 eV is given [7].

The LIF ion velocity distributions measured in the processing region show a distinct bimodal nature which is divided into a fast component and a slow component. The fast component is reported to arise from those ions which follow the magnet flux lines from the source into the reaction chamber; whereas, the slow component arises from those ions created where the source expands into the reaction chamber. The ion velocity distribution functions are nearly isotropic in the source region but become strongly anisotropic in the processing region as they follow electrostatic fields [12].

Chapter 3

LIF Apparatus/Multipolar ECR Plasma System

3.1 Introduction

This chapter introduces the specific equipment used to carry out the research described in this thesis. First the MPDR and its supporting equipment is described. The final sections detail the lasers, optics and signal collection equipment used for the laser induced fluorescence work.

3.2 Multipolar ECR Plasma System

The multipolar ECR source consists of a seven inch microwave cavity, the baseplate and the quartz cavity (Figure 3.1 and Figures 3.2a/b). The microwave cavity is a cylindrical resonant cavity which can be tuned with a sliding short. It directs intense microwave energy into the plasma source region. The baseplate contains the eight gas inlets and also a ring of eight rare earth magnets (Figure 3.2a). Each magnet measures two inches by one inch by one inch. These magnets create the ECR zones within the quartz cavity. A detailed description of the MPDR is found in reference [26].

3.2.1 The MPDR Baseplate

The baseplate, shown in Figures 3.2a and 3.2b, was designed to allow laser access to the plasma source region [27]. The plasma is created within a fused quartz chamber (Figure 3.2b) that is attached to the baseplate. The eight rare earth magnets are housed in a high permeability iron

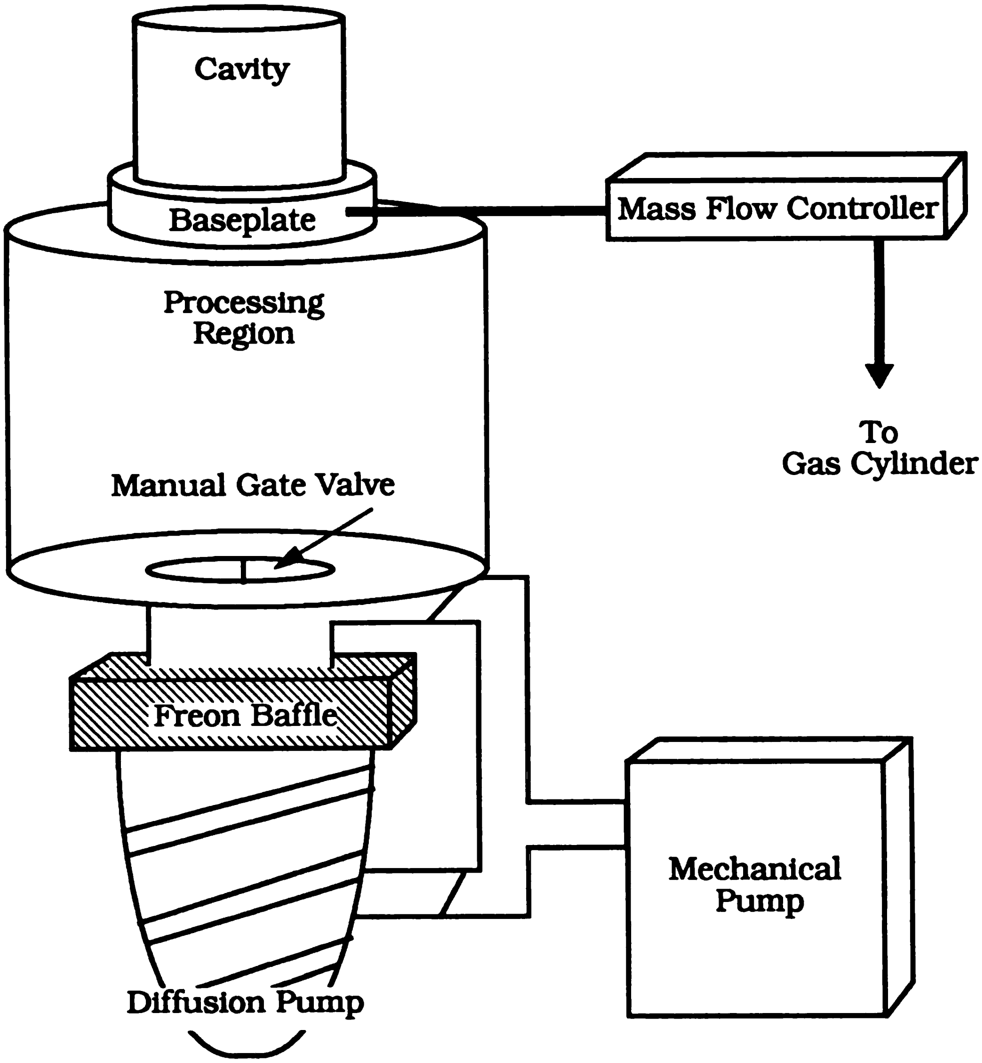

Figure 3.1: Cavity, Baseplate, Vacuum and Gas Systems

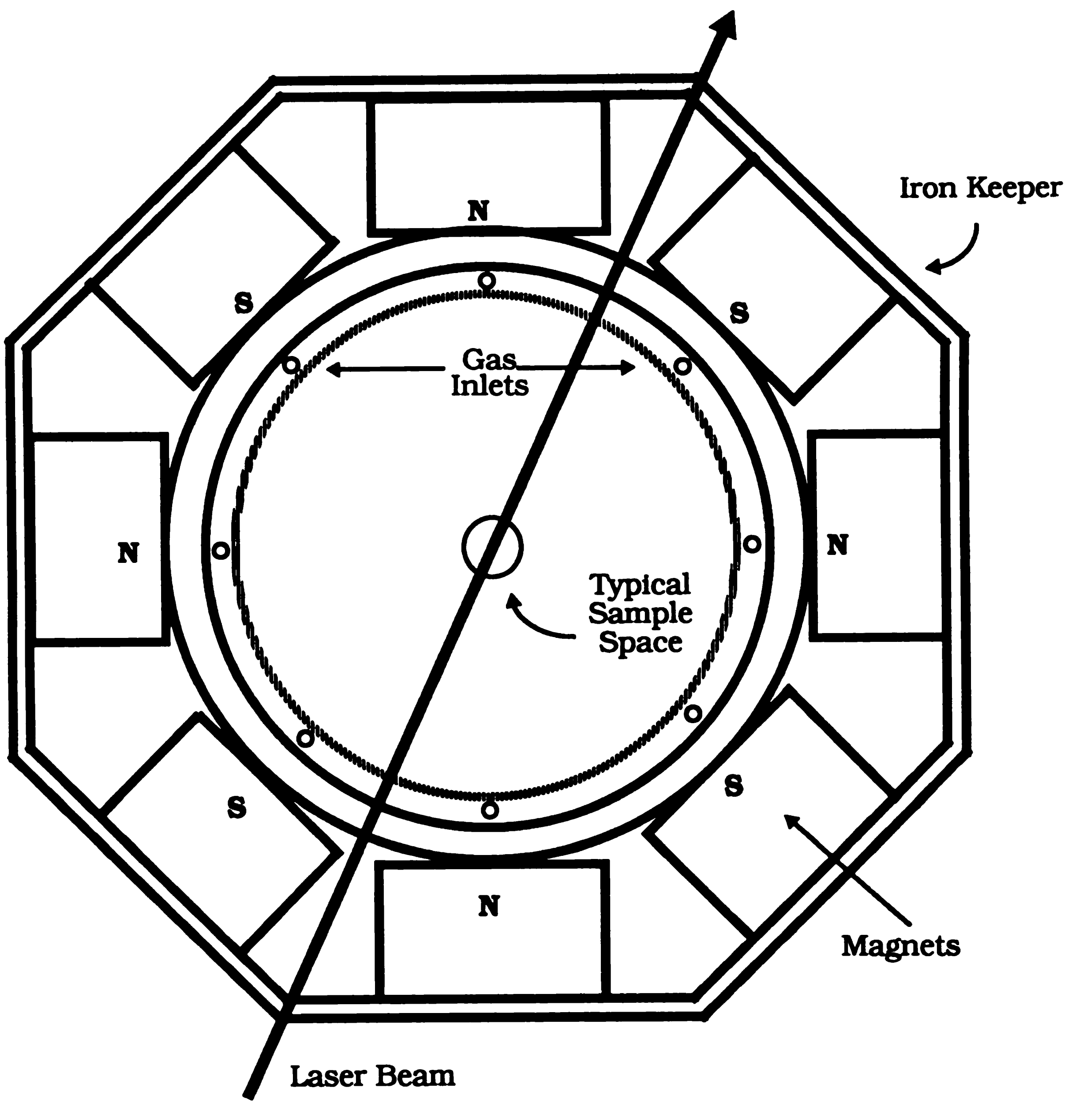

Figure 3.2a: MPDR Baseplate - Top View

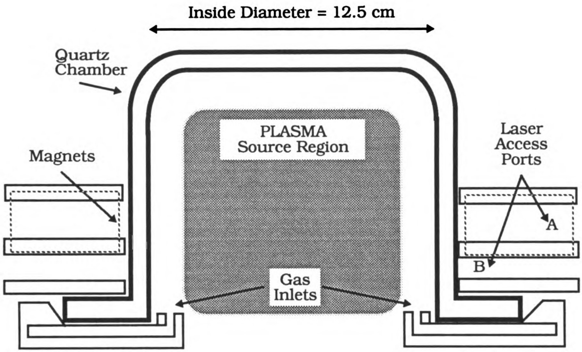

Figure 3.2b: MPDR Baseplate - Side View
Laser Port A is 2.5 cm high
Laser Port B is 0.6 cm high
Dashed Line Indicates Magnet Locations

keeper which focuses the magnetic fields within the quartz chamber and eliminates magnetic fields in the downstream processing region. These magnets have a low Curie temperature and therefore need cooling to protect them from the relatively high temperature of the plasma. Water cooling is provided by that section of the baseplate which surrounds the magnet ring. The baseplate design keeps the function of the iron keeper and the water cooling intact while allowing laser access to the discharge region in front of the magnets. The baseplate also serves as the mechanism for the distribution of the working gas into the chamber. Eight pinholes are arranged around and below the inner side of the quartz chamber for gas access. Also, air cooling is available for the quartz chamber if necessary.

3.2.2 The Microwave Subsystem

Microwave energy is supplied by a 2.45 GHz microwave power supply (Micro-Now 420B1). The experiments described here were performed with microwave power ranging from 150 Watts to 300 Watts. This power range refers to the power absorbed by the cavity which is found by subtracting the microwave power reflected by the cavity from the power incident on the cavity. The nominal value used was 250 Watts with less than 0.3% reflected. The microwave circuit, shown in Figure 3.3, includes the three port circulator and dummy load to protect the power supply and the dual directional coupler for sampling both the reflected and incident power.

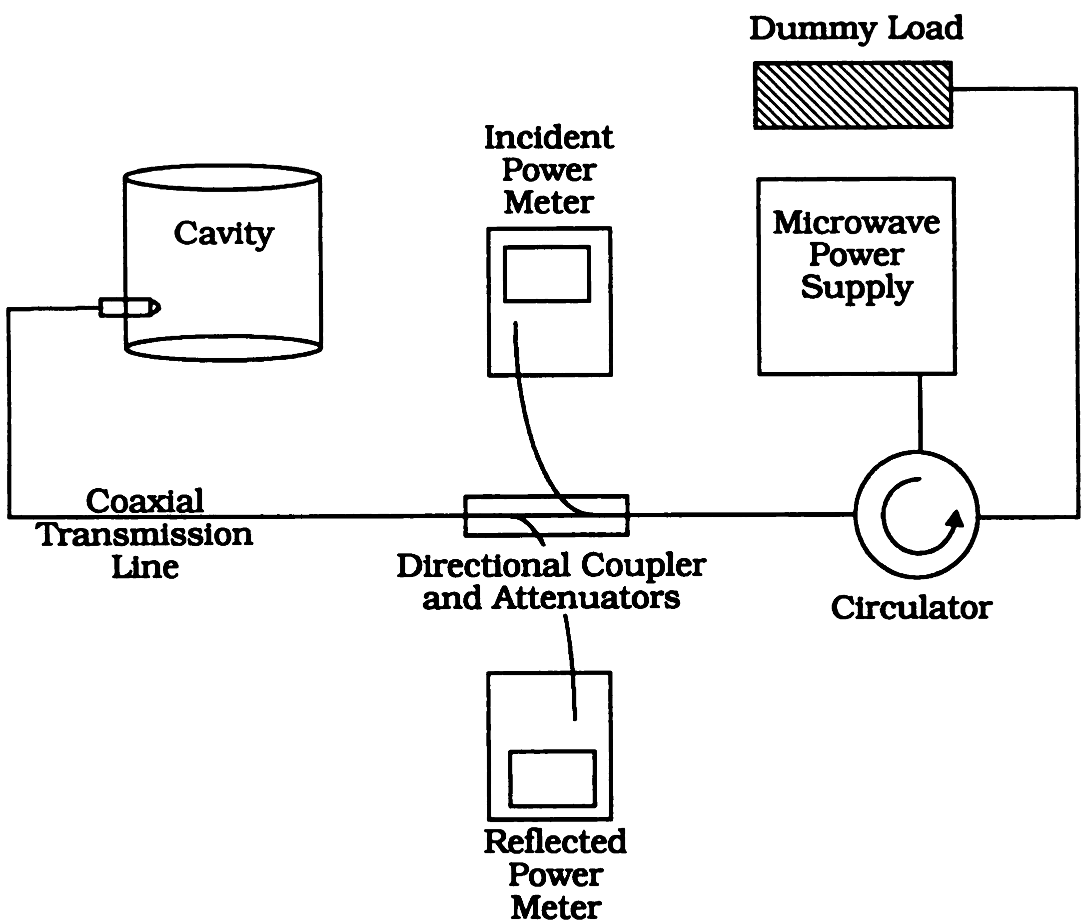

Figure 3.3: Microwave Subsystem

3.2.3 Gas/Vacuum Subsystems

The 99.999% pure Argon gas is fed into the baseplate through a mass flow controller (Tylan FC-280) with a range of flow from 10 to 30 sccm. The nominal value used is 20 sccm. The vacuum system includes a 2500 l/sec oil diffusion pump and a 33 m^3/sec mechanical pump both filled with a hydrocarbon-free oil to allow the use of reactive gases. To reduce backstreaming of oil, a freon-cooled baffle separates the processing chamber from the diffusion pump. This minimized the contaminates in the chamber at the expense of pumping speed.

A manual high-vacuum gate valve separates the diffusion pump from the processing chamber and allows manual throttling of the chamber pressure. The pressure is measured in the chamber with a capacitive manometer (MKS-390HA) down to about 1×10^{-5} Torr. Also, an ionization pressure gauge is located at the opening to the diffusion pump but the sensitivity of this instrument to non-nitrogen environments brings its accuracy into question. The vacuum and gas systems are represented schematically in Figure 3.1.

3.3 The Lasers

A number of different lasers could be chosen for LIF work each having distinct advantages. The laser chosen, though, must have high peak power, a narrow spectral width and be frequency tunable. The work presented in this thesis uses a tunable dye laser pumped by a Nd:YAG pulsed laser. The complete LIF apparatus is shown schematically in Figure 3.4.

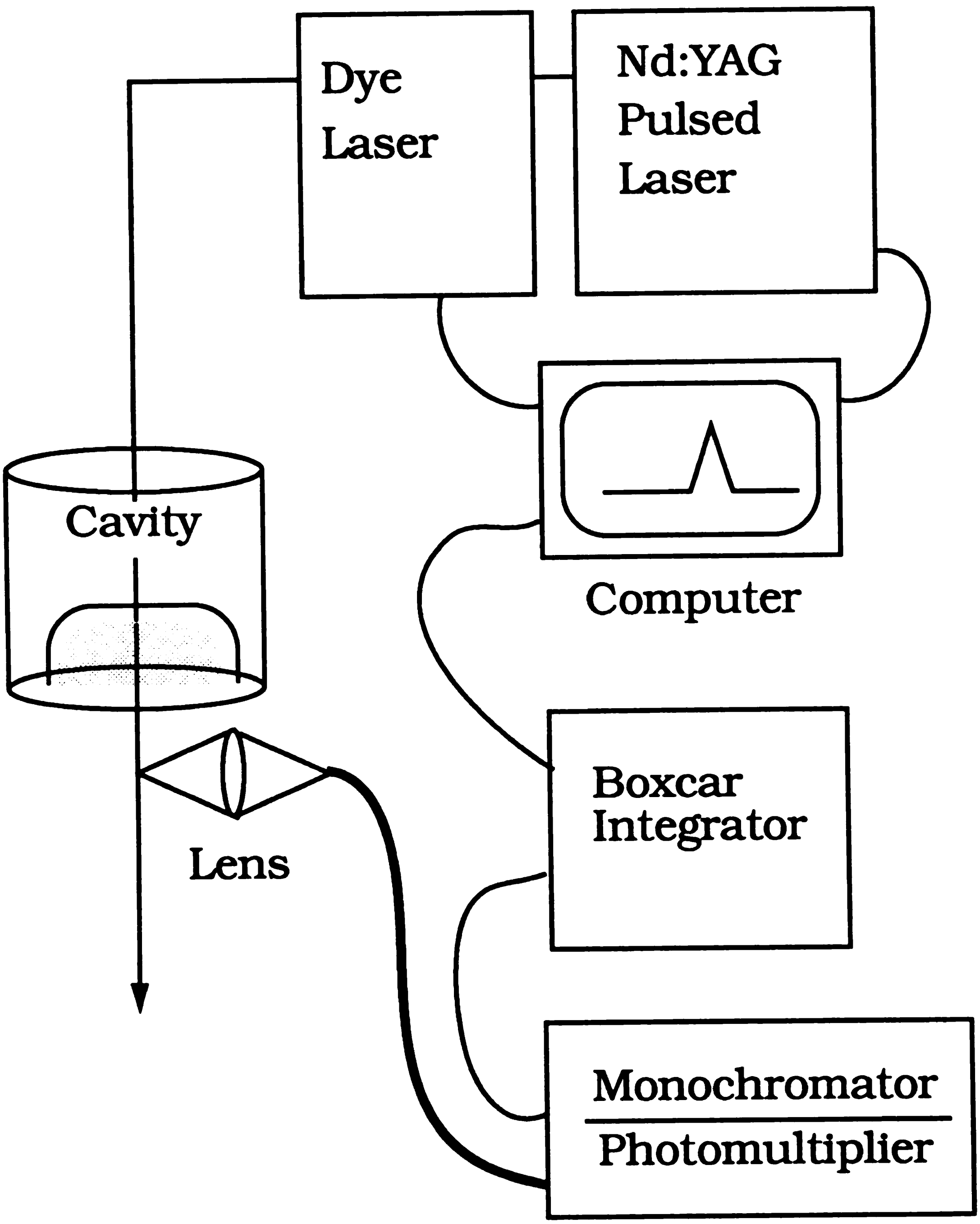

Figure 3.4: The Laser System

3.3.1 Nd:YAG Pulsed Laser

In order to adequately pump the dye laser and increase the signal to noise ratio by minimizing the loss of excited species due to quenching, saturation of the laser induced absorption transition should be assured (Section 2.2.1). One way to saturate this transition is through the use of a high power laser. The necessary high power is achieved with a Q-switched neodymium doped yttrium aluminum garnet (Nd:YAG) pulsed laser (Spectra-Physics DCR-11). The peak power of 40 MWatts with a pulse duration of 6 nsec assures adequate pumping of the lossy tunable dye laser after frequency doubling to facilitate saturation of the absorption transition.

The laser output of the pump laser is frequency doubled using an harmonic generator (Spectra-Physics HG-2). The harmonic generator consists of a KD*P crystal (potassium dideuterium phosphate) which interacts with the fundamental 1064 nm light from the Nd:YAG laser to produce a secondary wave with half the wavelength. Since the conversion efficiency of the crystal is highly dependent on its temperature, a temperature controller is necessary for optimum frequency conversion.

3.3.2 Dye Laser

Since many suitable transitions exist and many different gases can be used, a tunable laser is necessary to fully analyze any plasma system. The dye laser as used in this work (Spectra-Physics PDL-3) provides tunable laser radiation from 380 nm to 960 nm.The particular range of laser radiation available depends on the dye used. In order to scan the entire velocity distribution of the particular argon species studied here (624.3 nm), Exciton DCM dye was chosen.

In addition to the dye, the angle of the wavelength tuning grating is adjustable to permit spectral tuning of the output radiation. Control of the grating angle is achieved through the use of a stepper motor and stepper motor controller. A personal computer is used to coordinate the motor, the light collection stages and the gated integrator.

3.4 Fluoresced Light Collection

Laser access to the plasma is achieved as described in Section 3.2.1. This section will describe the collection of the fluoresced light and the apparatus necessary for spatial characterization of the ion species.

3.4.1 Optics

Emitted light is collected by a lens of diameter 6.3 cm and focal length 5 cm. The light is focused onto a 1 mm diameter fiber cable which carries the light out of the vacuum system to the monochromator. The imaging system just described is shown in Figure 3.5 along with the translation stages necessary to move the focal point within the vacuum. Three dimensional movement is available with the three translation stages which allows precise positioning of the collection volume along the laser beam. The x and y stages allow movement along a distance of 4 inches and the z stage allows movement along 2 inches.

Figure 3.5 also shows the actual spatial dimensions of the collection volume and gives an estimate of the spatial resolution of the system as used in this work. The sample volume is 0.05 cm^3 in this configuration. Using a calculation of the solid angle subtended by the optics and assuming fluorescence occurs isotropically, about 1% of all photons emitted are collected by the lens.

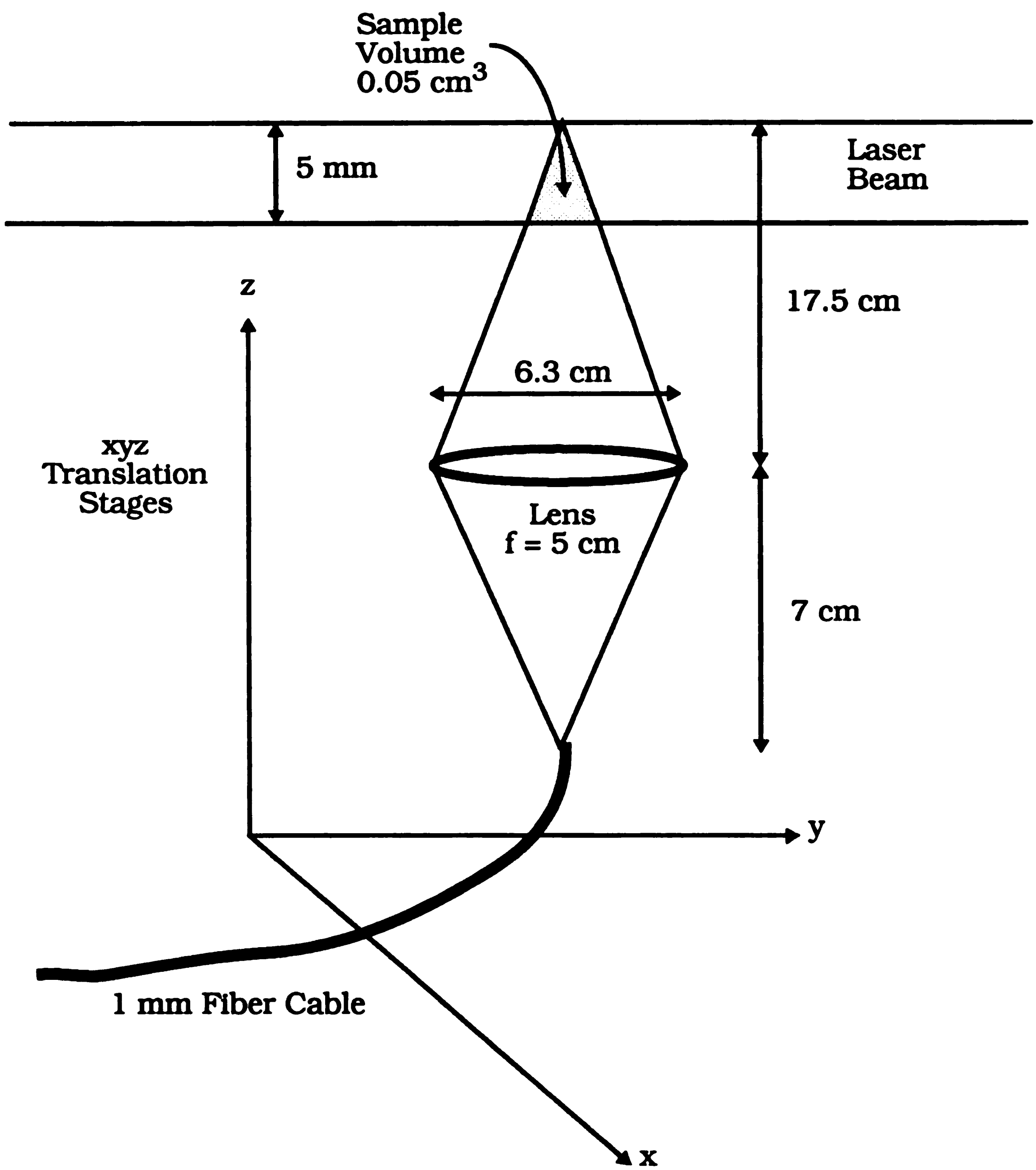

Figure 3.5: Optics and Spatial Resolution

3.4.2 Monochromator

A 1 meter, f/9, Spex, Inc. monochromator is used to filter unwanted light from the fluorescence signal. In addition, an optical filter with a passband centered near the fluoresced light wavelength is used to further reduce the amount of unwanted light affecting the signal. The light from the monochromator is detected using an EMI, Inc. cooled photomultiplier. The monochromator entrance and exit slits are set at 1 mm to ensure good signal to noise ratio. Since the spectral resolution of the apparatus is determined by the laser linewidth and other broadening mechanisms the spectral width of the monochromator is not a factor.

3.5 Gated Integrator

A gated or boxcar integrator (EG&G PARC 4121B) is used to repetitively sample the fluorescence signal emanating from the photomultiplier. The integrator samples the photomultiplier signal when triggered by the pump laser. The samples are averaged to improve the signal to noise ratio (SNR). The averaged signal is converted to a digital signal to allow data collection by computer using an A/D converter (EG&G PARC 4161A).

A preamplifier is in place between the photomultiplier tube (PMT) and the gated integrator. The charge sensitive amplifier shown schematically in Figure 3.6 is DC coupled to the gated integrator [28].

The important aspect of the gated integrator set-up is the timing of the trigger with respect to the laser pulse. In order to minimize any stray laser light from artificially enhancing the fluorescence signal, the integrator is timed to collect fluoresced light immediately after the end of the laser pulse. Figure 3.7 shows a timing diagram where the laser pulse,

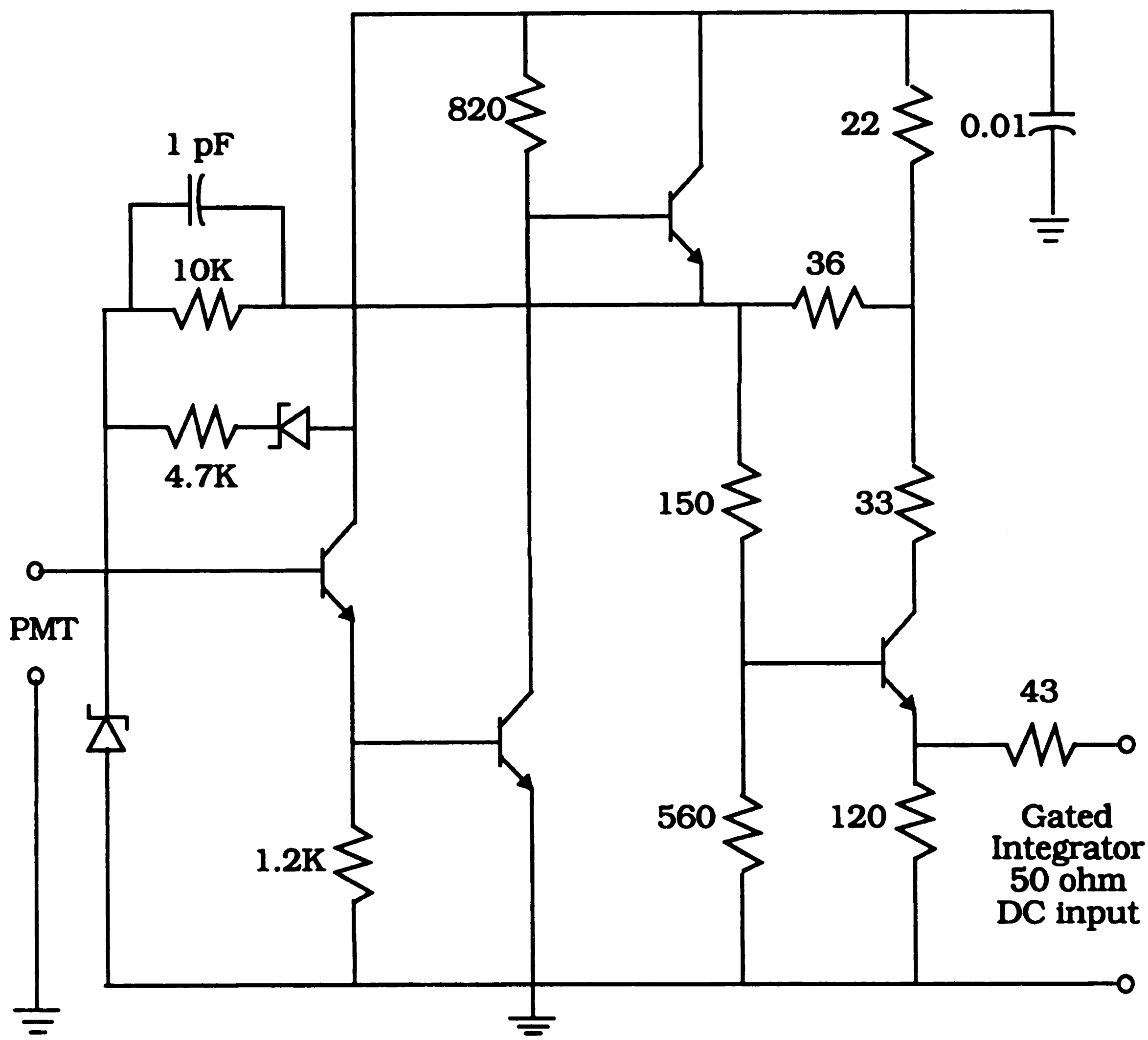

Figure 3.6: Photomultiplier Signal Amplifier

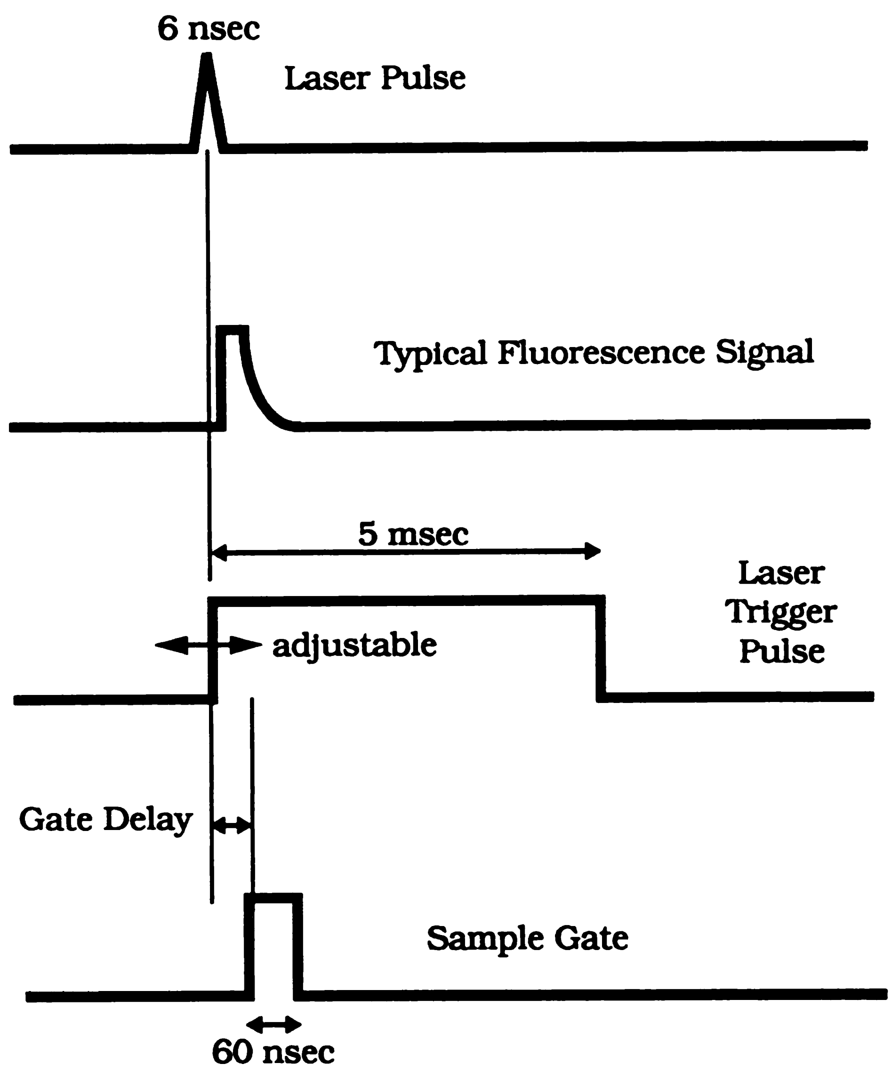

Figure 3.7: Gated Integrator Timing Diagram

trigger pulse, fluorescence pulse and the open gate of the integrator are shown. Two timing adjustments are possible. The delay between the actual laser pulse and the start of the trigger pulse is adjustable (shown in Figure 3.7). Also, a more sensitive adjustment is available on the gated integrator which allows control of the delay between the time the gated integrator receives the trigger and the start of the gate (Gate Delay in Figure 3.7). In this work, a gate of 60 nsec with 30 samples averaged using an input signal sensitivity of 200 mV is found to give the best signal strength without serious SNR problems and is used for most of the measurements.

3.6 Computer Control

The entire experiment is controlled through the use of an IBM PC computer with various interface boards. LIF signals are determined by first pulsing the laser for a prescribed number of seconds and simultaneously collecting the gated integrator signals. Then the measuring process is repeated for the same length of time with no laser pulses. By comparing the gated integrator signals when the laser is pulsing to the background signals when the laser is off, the LIF signal strength is determined. Generally, at each wavelength point the intensity shown is an average of 7 to 13 on-off cycles where each cycle is about 18 sec each.

The computer also controls the dye laser grating through the stepper motor and stepper motor controller. Additionally, movement of the collection optics is achieved through control of the translation stages within the vacuum chamber. The complete QuickBasic program used for computer control is included in the Appendix.

Chapter 4

Ion Energies and Velocities

4.1 Introduction

The implemented LIF system has been tested by applying it to the study of ion energies and velocities in an MPDR plasma. The MPDR system has been split into two distinct regions. The source is that region within the discharge chamber where the plasma is generated and electromagnetic energy is coupled to the electron gas by the electric fields of the microwave cavity and the ECR static magnetic fields. The processing region lies below the source as in Figure 4.1 and is where the ion energy and velocity distributions are dominated by plasma potential gradients and diffusion processes from the source to the processing regions.

Since the ion energies along the laser direction are measured, changing the direction of the laser provides information on the distributions both horizontally, with a radial laser beam, and vertically, with a longitudinal laser beam as shown in Figure 4.2. Ion energy distributions are measured in both regions and, within the source region, in both directions. Ion velocity distributions are particularly interesting when comparing one position with another and therefore they are presented in that context.

The study described here concentrated on demonstrating the implementation of an LIF system to study a singly ionized argon metastable in an ECR plasma. Specifically the absorption transition is the $3d^4F_{7/2}$-$4p^2D_{5/2}$ transition at 624.3 nm. The emission is the $4p^2D_{5/2}$ - $4s^2P_{3/2}$ transition at 488.0 nm.

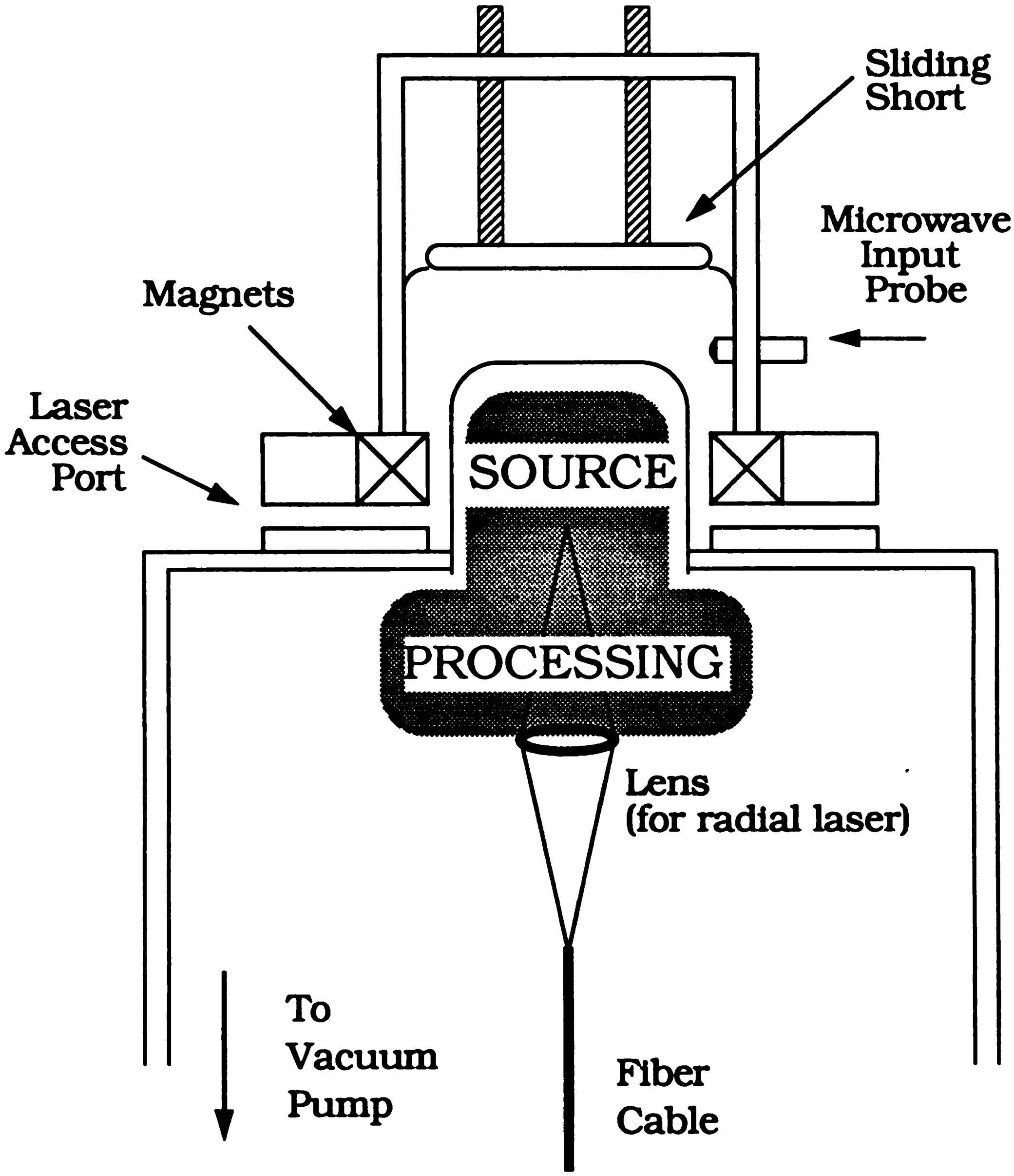

Figure 4.1: Source and Processing Regions

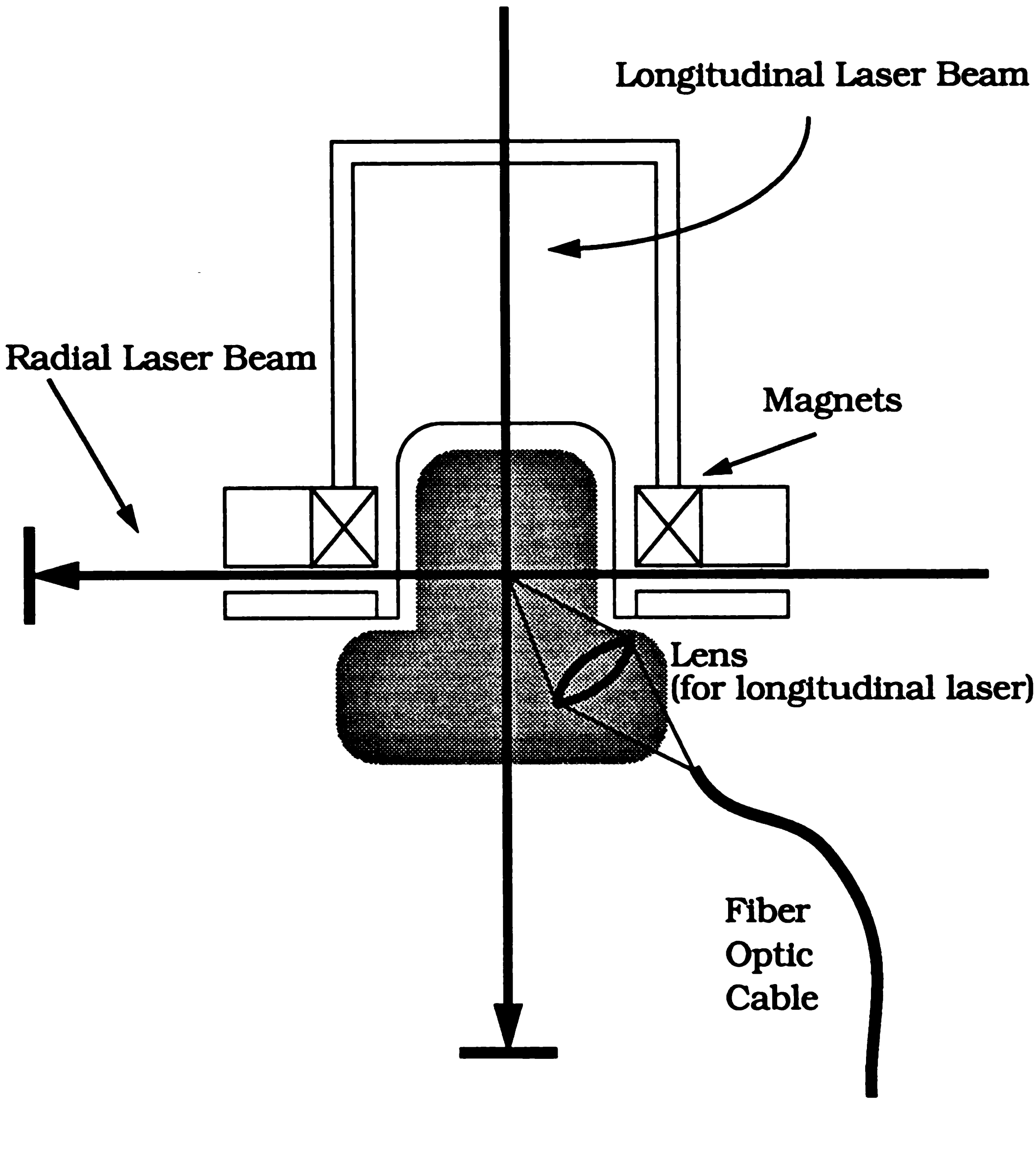

Figure 4.2: Longitudinal and Radial Laser Beam

4.2 Spectral Line Broadening

A typical ion energy distribution, measured at the center of the source region (r=0, z=1: Figure 4.3), is shown in Figure 4.4 where fluorescence intensity in arbitrary units (arbs) is measured versus ion velocity. An obvious feature of this distribution is that it has a certain non-zero width. A number of factors contribute to the broadening of the distribution, including Doppler shifts, high laser power, laser spectral width, magnetic fields and electric fields. Therefore, care must be taken in interpreting the results.

4.2.1 Doppler Broadening

Doppler shifted broadening (Sections 2.2.2 and 2.2.3) occurs due to the relative motion of the ion with the observer. From an assumed Gaussian distribution a full width at half maximum is found which relates the average ion energy or temperature to the observed distribution (Equation 2.5). This is an actual temperature only in the absence of all other broadening mechanisms.

4.2.2 Laser Broadening

Laser broadening occurs due to the non-zero linewidth of the laser light. If the laser light is Gaussian and a Doppler-broadened line takes a Gaussian shape then the two can be deconvolved [7].

$$\Delta\lambda_{dop} \approx \sqrt{(\Delta\lambda_{obs})^2 - (\Delta\lambda_{las})^2} \qquad (4.1)$$

where $\Delta\lambda_{dop}$ is the Doppler broadened FWHM, $\Delta\lambda_{obs}$ is the FWHM of the

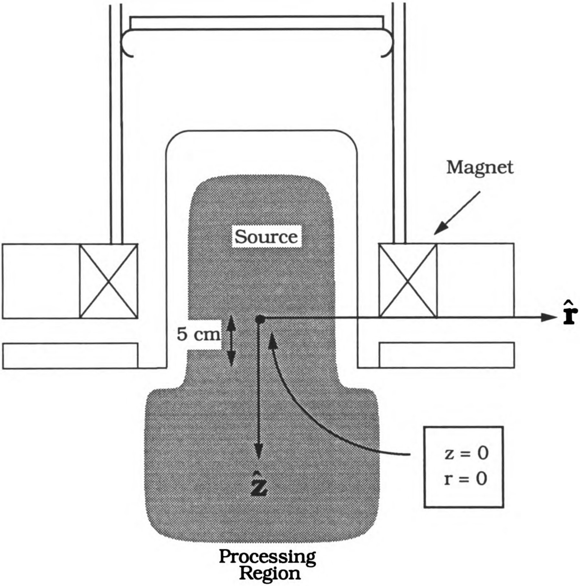

Figure 4.3: Geometry within Source and Processing Regions

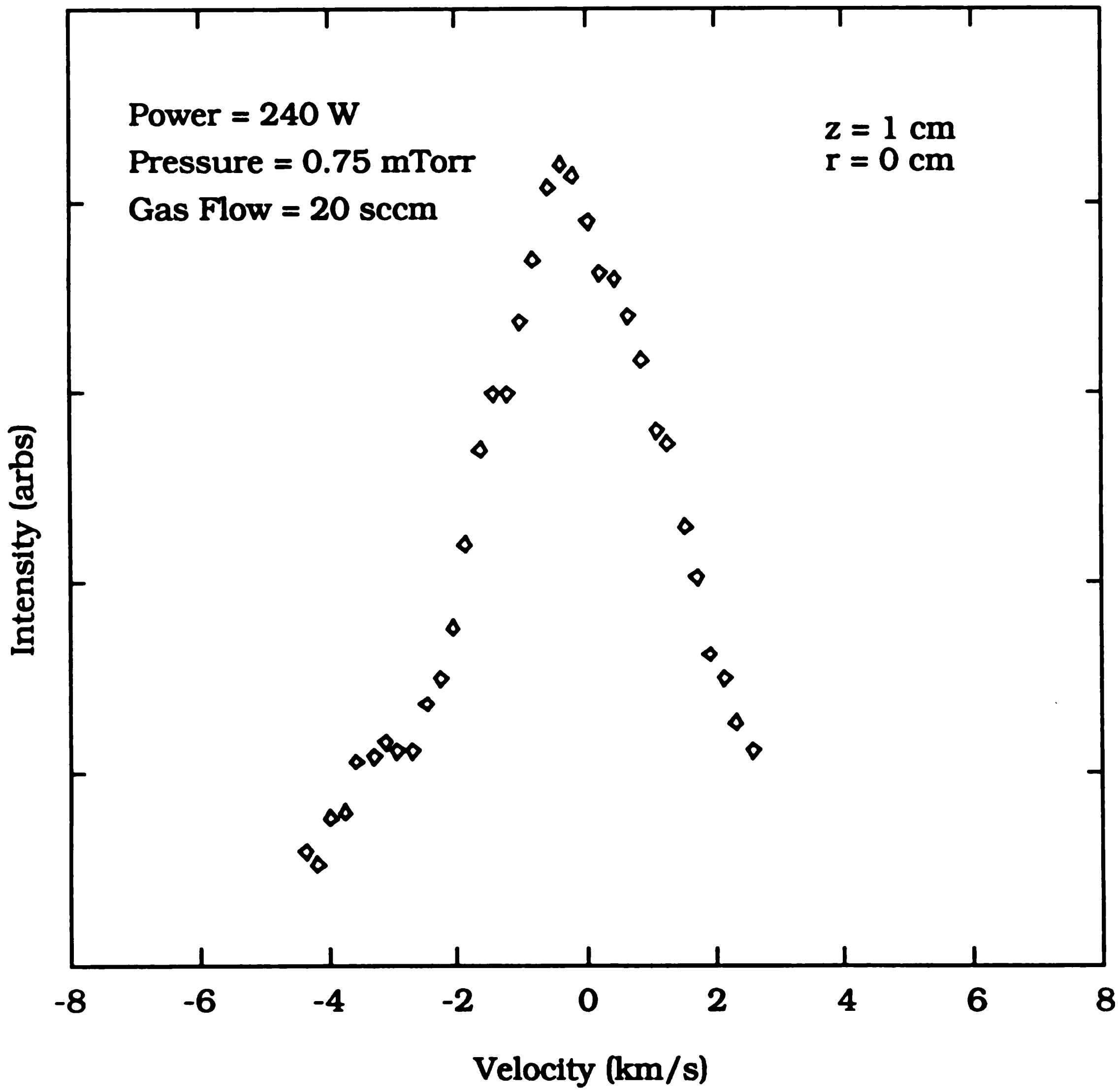

Figure 4.4: Radial Velocity Distribution in Source Region

observed line and $\Delta\lambda_{las}$ is the linewidth of the laser. Equation 4.1 is used to extract a Doppler broadened linewidth from the observed line when all other broadening mechanisms are minimized.

4.2.3 Zeeman Splitting

Zeeman splitting is the effect of magnetic fields on the observed distribution. It is not broadening in the sense of Doppler broadening but actually arises as the splitting of the spectral absorption energy into two or more distinct energies. For most of the locations inside the plasma region measured in this thesis, the magnetic fields are negligible and Zeeman splitting can be ignored. Reference [27] shows that the magnetic fields in most of the sample areas are negligible, particularly at the center of the source and processing regions.

4.2.4 Power Broadening

Line broadening due to the power density of the laser is termed power broadening. The pulsed laser used in these experiments operates at a power density such that power broadening is observed. In order to reduce the effect of power broadening, the laser intensity is attenuated using a series of optical density filters.

The power broadening effect is determined by taking a series of measurements with increasing attenuation of the beam. As the attenuation increases the broadening of the line decreases until the power broadening is negligible compared to the Doppler broadened line. The beam was attenuated using a series of optical density filters placed in the path of the laser. The crucial ion energy measurements were taken at this incident laser power. In the interest of signal to noise certain relative measurements were taken without attenuation of the laser.

4.3 Ion Energies

The ion energy distribution in Figure 4.4 is found at the center of the source region (r=0, z=1 on Figure 4.3) with a radial laser beam. The resolved ion energy is found to be about 0.5 eV after reducing the laser power to minimize power broadening, deconvolving the laser broadening and verifying negligible magnetic fields. Due to residual power broadening this is set as an upper limit until further research refines the measurement.

Figure 4.5 shows a similar distribution where the sample space is located at the same point (r=0, z=1). This distribution is taken with a longitudinal laser beam and the light collection optics set at an angle greater than ninety degrees (see Figure 4.2 for laser beam direction and optics set-up). The upper limit ion energy in this case is also 0.5 eV with the same experimental parameters as Figure 4.4.

4.4 Ion Velocities

Ion velocity distributions are found using the techniques described in Section 2.2.2. The velocity distributions are particularly interesting when comparing one location with another. Since the measurement is taken at the center of the source region the distribution of velocities is assumed to be random, therefore the peak of the distribution is chosen as the zero velocity point.

The geometry used to describe the MPDR system is shown in Figure

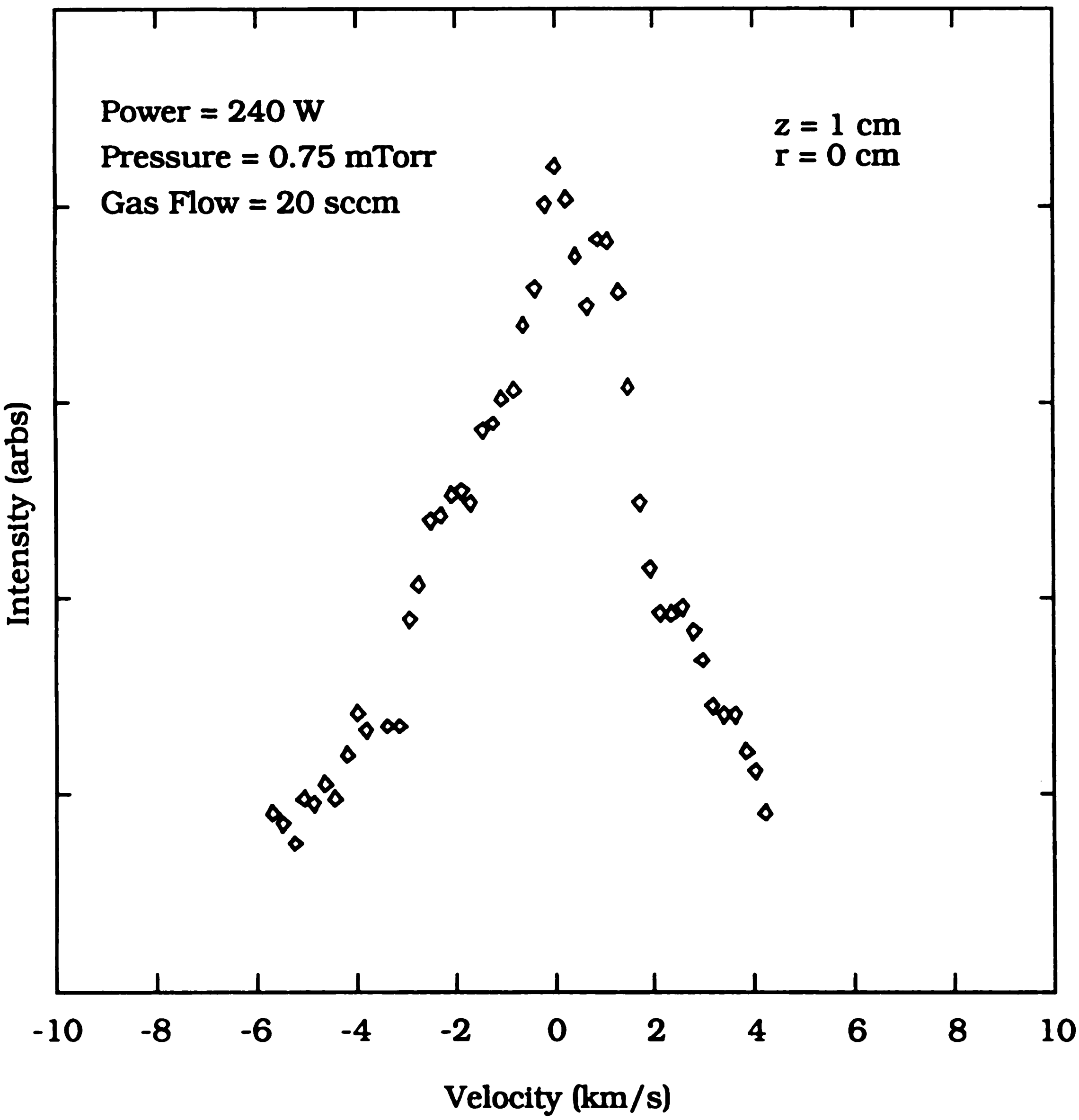

Figure 4.5: Longitudinal Velocity Distribution in Source Region

4.3 where the center point of the source region is chosen as the origin of polar coordinates ($r = 0$, $z = 0$). Longitudinally, this point lies at the base of the magnets and radially, at the center of the quartz chamber. The positive longitudinal direction is from the source to the processing region. The positive radial direction is from the origin out to the magnets.

Figure 4.6 shows a series of velocity distribution measurements taking at three different longitudinal positions. The important point to notice is the shift of peak ion velocity from source to processing region. This indicates the ions have picked up a directed energy component as they leave the source. If the peak velocity of an ion at $z = 1$ cm is taken as the reference then the peak velocity at $z = 3$ cm is 1.24 km/sec and at $z = 5$ cm is 2.02 km/sec. This shows an increase of 2 km/sec over 4 cm.

4.5 Conclusions

The operation of the LIF system for determining ion velocities has been demonstrated. In some initial test measurements, the ion energy within the source region is given an upper limit of 0.5 eV regardless of laser direction at a pressure of 0.75 mTorr with 240 Watts of microwave power and an argon gas flow of 20 sccm. This is only an upper limit since residual line broadening of those distributions shown in Figure 4.4 and Figure 4.5 may still be a factor.

The ion velocity distributions given indicate a directed energy component from source to processing region. This indicates a change in plasma potential between the points of the measurement. The data indicates an increase in directed ion energy of about one electron volt. This corresponds to a potential variation over the 4 cm measured from one cm to

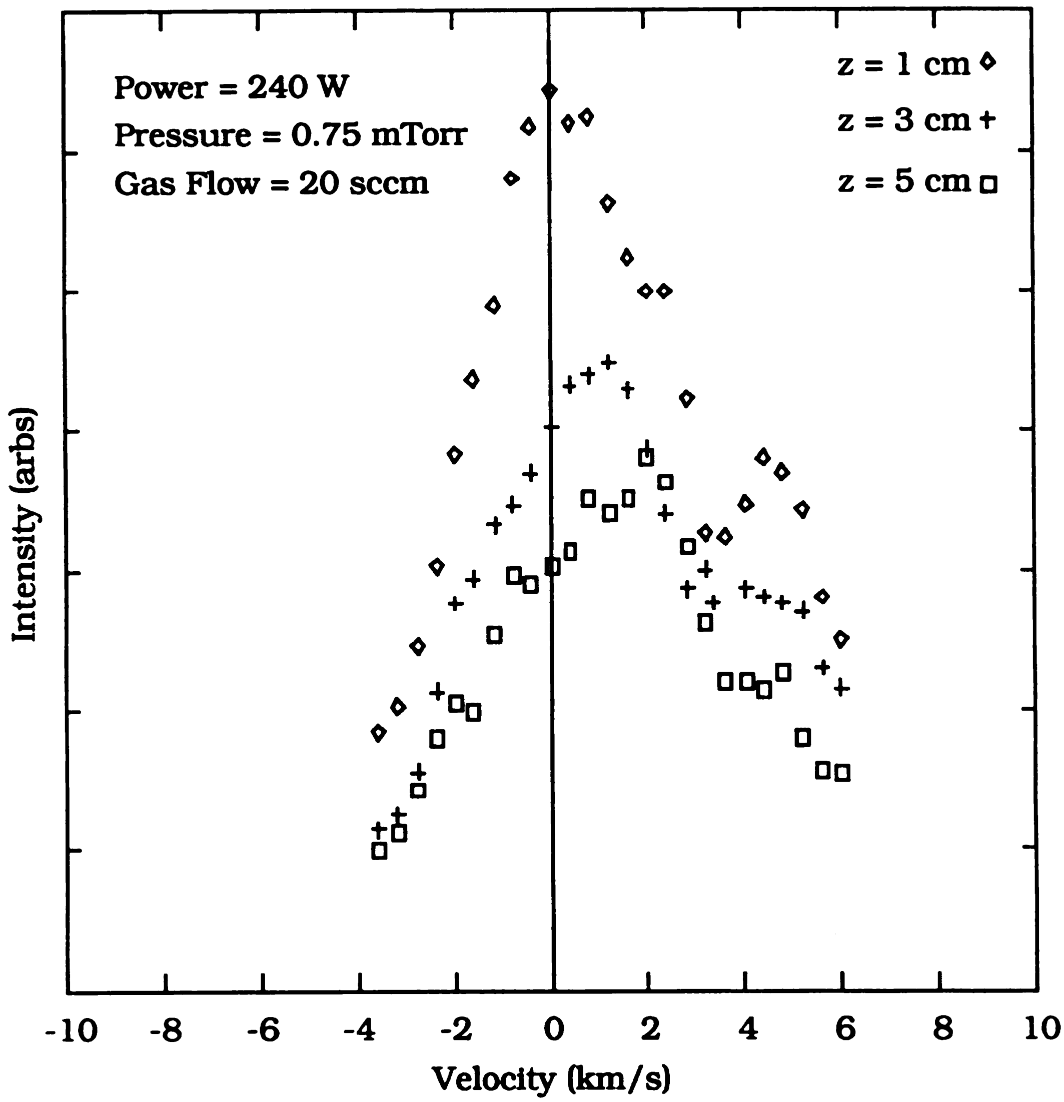

Figure 4.6: LIF Spectra at Various Longitudinal Positions

five cm below the magnets of less than 25 volts/meter at a pressure of 0.75 mTorr with 240 Watts of microwave power and an argon gas flow of 20 sccm.

Chapter 5

Relative Ion Densities

5.1 Introduction

Another interesting use of laser induced fluorescence is with regard to ion density measurements. LIF can give both relative and with proper calibration absolute density measurements. This section describes relative ion density variation measurements within the source region of the MPDR plasma. To evaluate the operation of the LIF system, selective comparisons are performed between the LIF measurements and double Langmuir probe measurements. The density measurements are with respect to microwave input power, chamber pressure and gas flow rate.

5.2 Relative Ion Density versus Microwave Power

Figure 5.1 shows the variation of the intensity of the laser induced fluorescence with increasing microwave input power from 150 - 290 Watts. The data shown are at two different locations within the plasma processing system as indicated in the figure. A longitudinal laser beam is used (Figure 4.2). The upper solid curve shows that the metastable species density increased as the microwave power increased. The lower solid curve shows a similar increase but at a slower rate.

The data presented in Figure 5.1 correlate very well with total ion density variation measured using a double Langmuir probe [27]. The increase in microwave power leads to more energetic particles in the ECR volumes and consequently more ionizations farther from these volumes

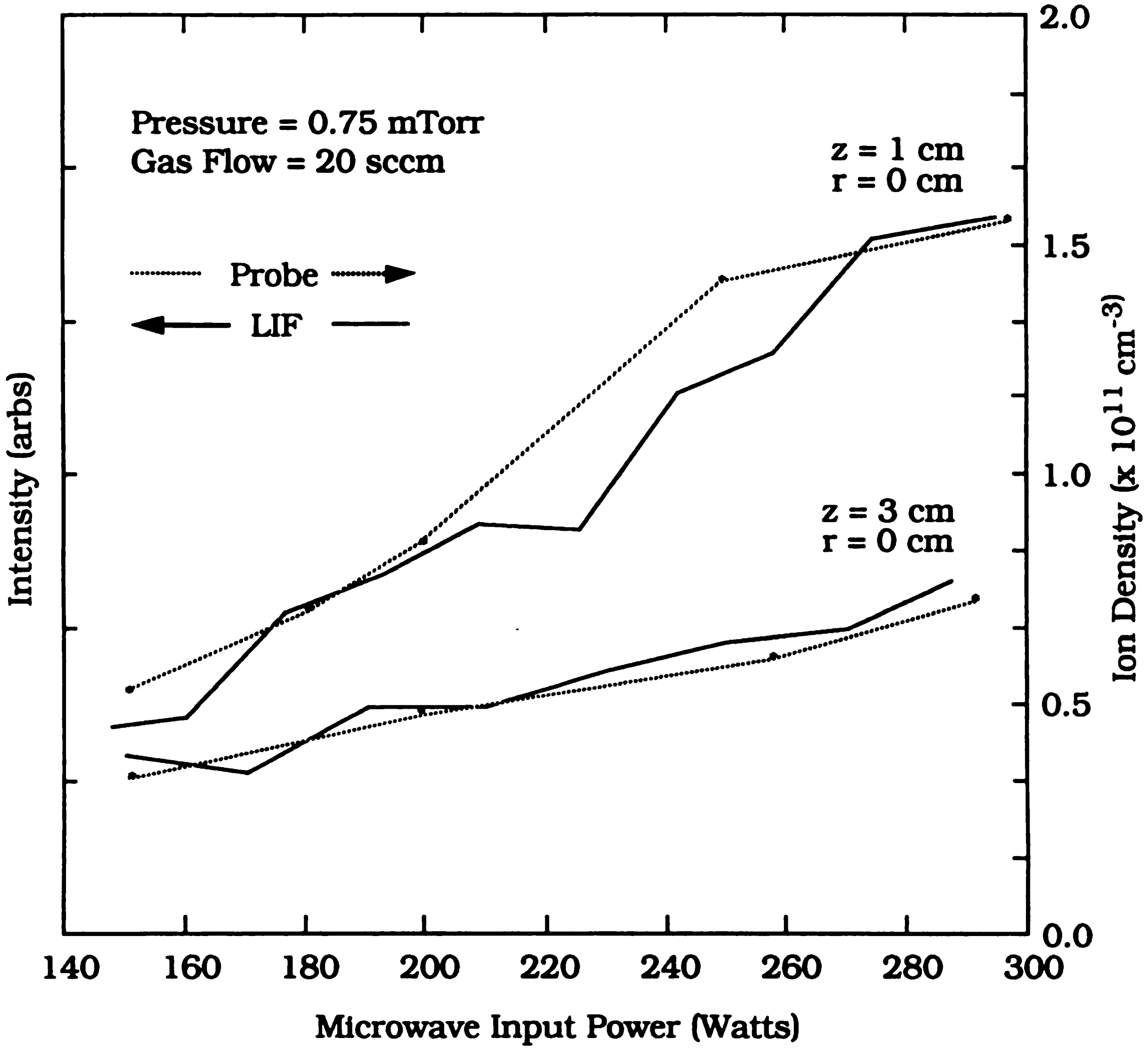

Figure 5.1: LIF Intensity versus Microwave Power

which is measured as a relative increase in metastable ion density in the case of LIF and an increase in total ion density in the case of the double Langmuir probe.

5.3 Relative Ion Density versus Gas Flow

Figure 5.2 shows the variation in LIF intensity with a change in gas flow rate from 10 sccm to 40 sccm. The pressure in the chamber is allowed to vary from 0.43 mTorr up to 1.31 mTorr as the gas flow increased. The ion density remains fairly constant throughout the range of gas flow tested indicating that a simple increase in neutral species does not necessarily increase ionizations. The likely affect is that the excess neutrals are simply removed from the region through the vacuum pumps. As expected, though, the relative ion density drops for measurements downstream from the ECR volumes.

5.4 Relative Ion Density versus Pressure

Figure 5.3 shows the relative change in metastable ion density as pressure is increased. The gas flow and the microwave power are kept constant throughout these measurements. The drop in LIF intensity as the pressure is increased can be attributed to the decrease in volume size of the neutral ionization region as the pressure is increased. At the higher pressures the majority of the ionizations are taking place in a smaller region which is close to the ECR volume. Also at the higher pressures, increased quenching may reduce the excited species density at locations away from the ionization regions. Therefore, at the center of the source (r=0) the LIF intensity drops since there are fewer excited species at this

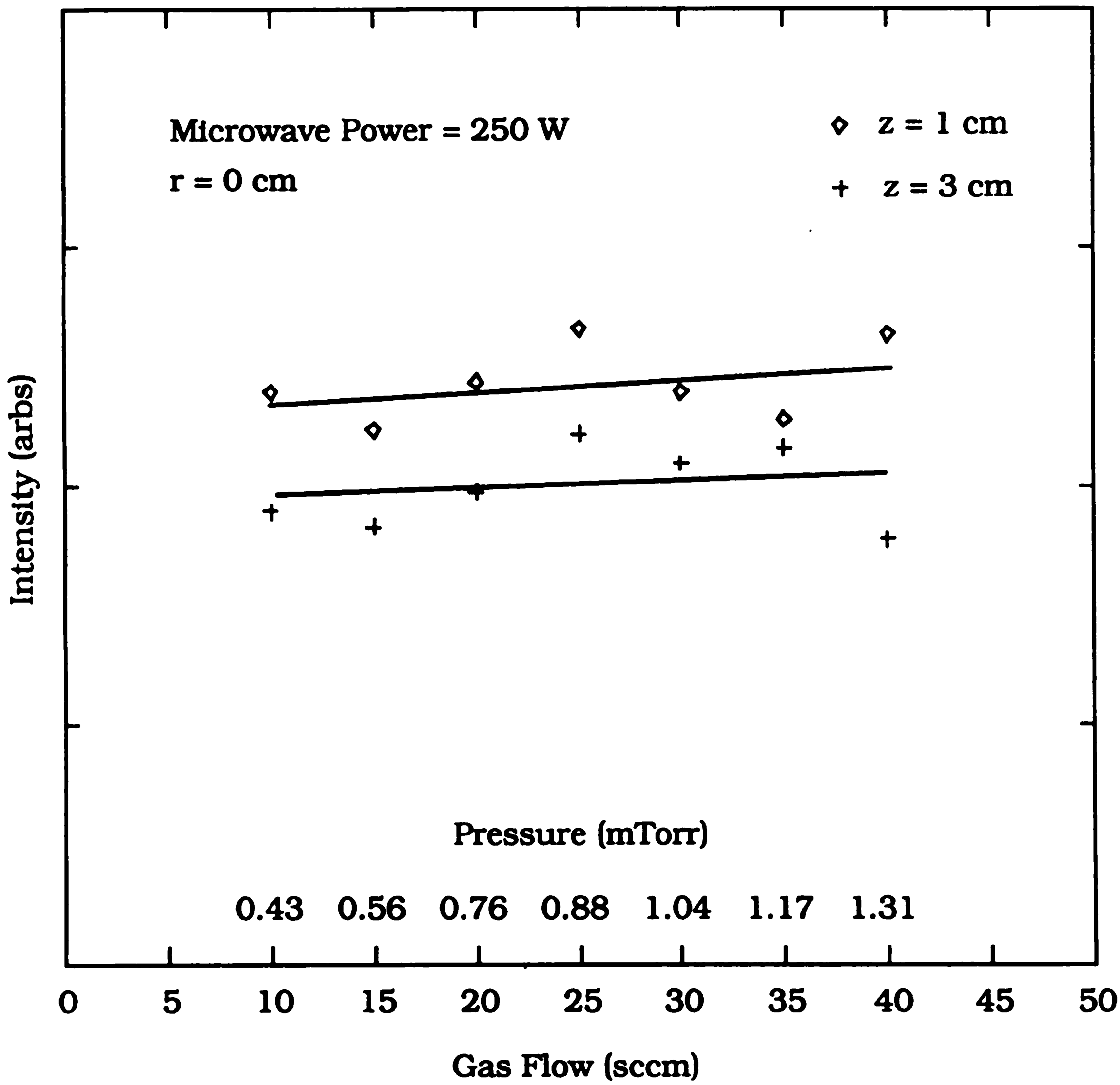

Figure 5.2: LIF Intensity versus Gas Flow

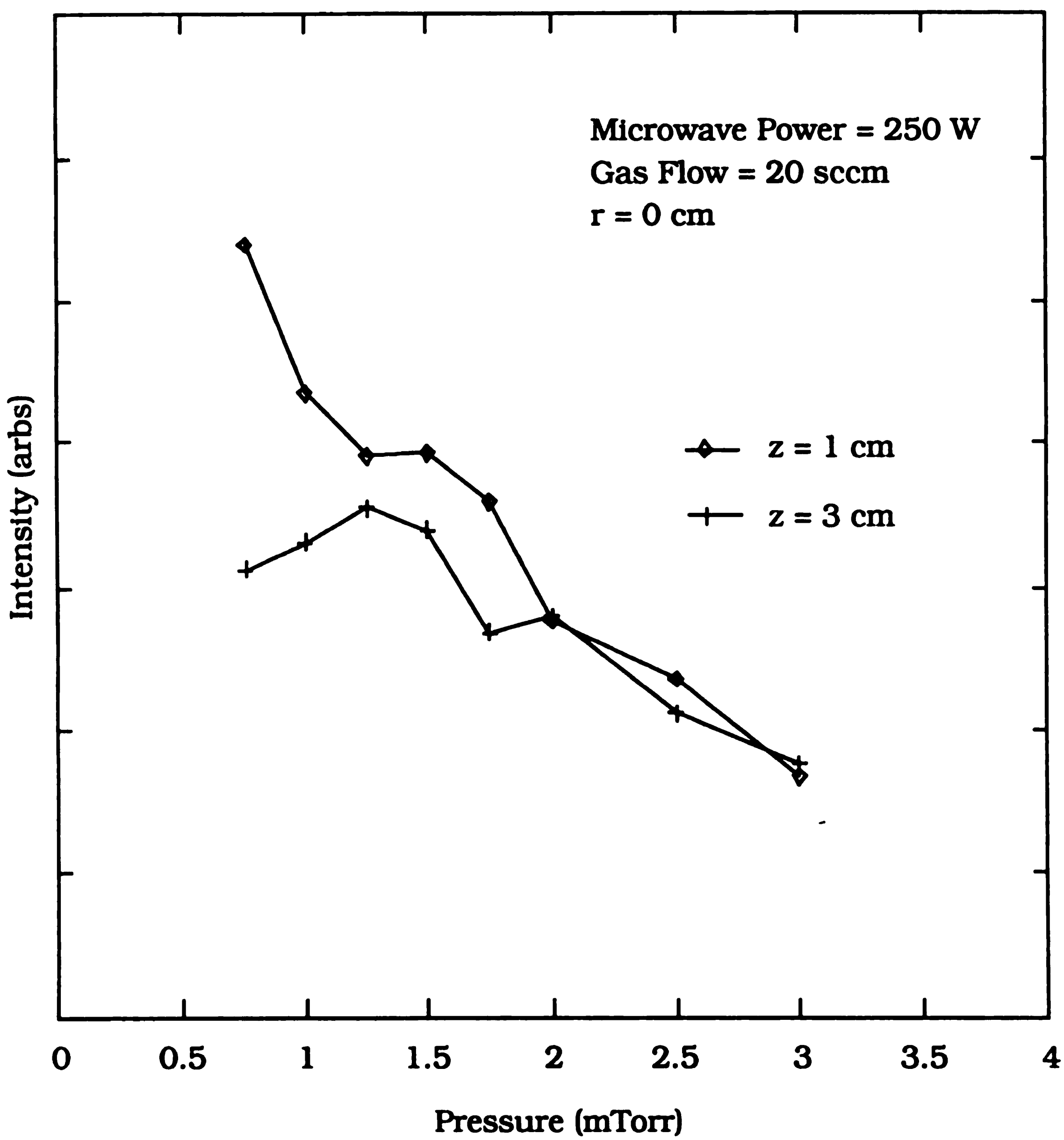

Figure 5.3: LIF Intensity versus Pressure

point. This is particularly evident at the higher pressures above 1.5 milli-Torr.

5.5 Relative Ion Density versus Radial Position

Figure 5.4 examines the change in relative ion density as the measurement volume moves closer to the ECR excitation volumes. These lines can not be used for energy measurements since the sample volume moved closer to the magnets and higher magnetic fields which produce Zeeman splitting. Interestingly, the measurement at r = 3 cm is taken just at the edge of a visibly bright region within the plasma source (shown in Figure 5.5 as the ECR volumes). The measurement indicates a substantial increase in metastable ion density which would correspond to an increase in excited species and therefore a brighter "light."

5.6 Conclusions

The LIF system has been tested by applying it to determine relative ion densities. These relative ion density LIF measurements indicate changes in ion density can be produced by changes in experimental reactor parameters. These measurements show an increased ion density with increased microwave power (150 W to 300 W) indicating more ionizations are taking place. This data corresponds well to the total ion density measurements taken with a Langmuir probe.

The relative metastable ion density decreases with increased pressure and constant gas flow indicating fewer excited species are present in the center of the source at the higher pressures tested (particularly over the 1.5 to 3 mTorr region). The measurements show little density change

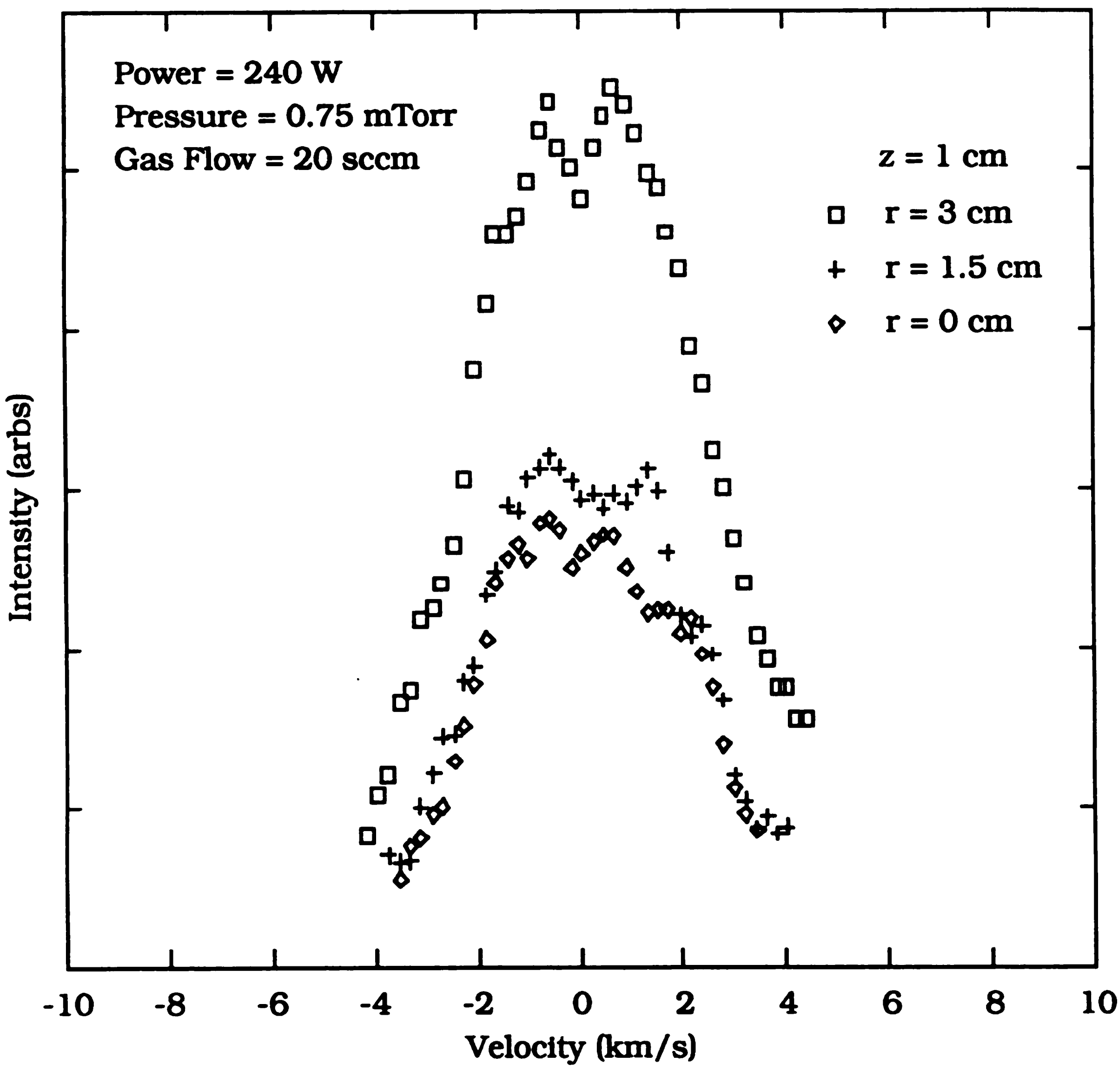

Figure 5.4: LIF Spectra at Various Radial Positions

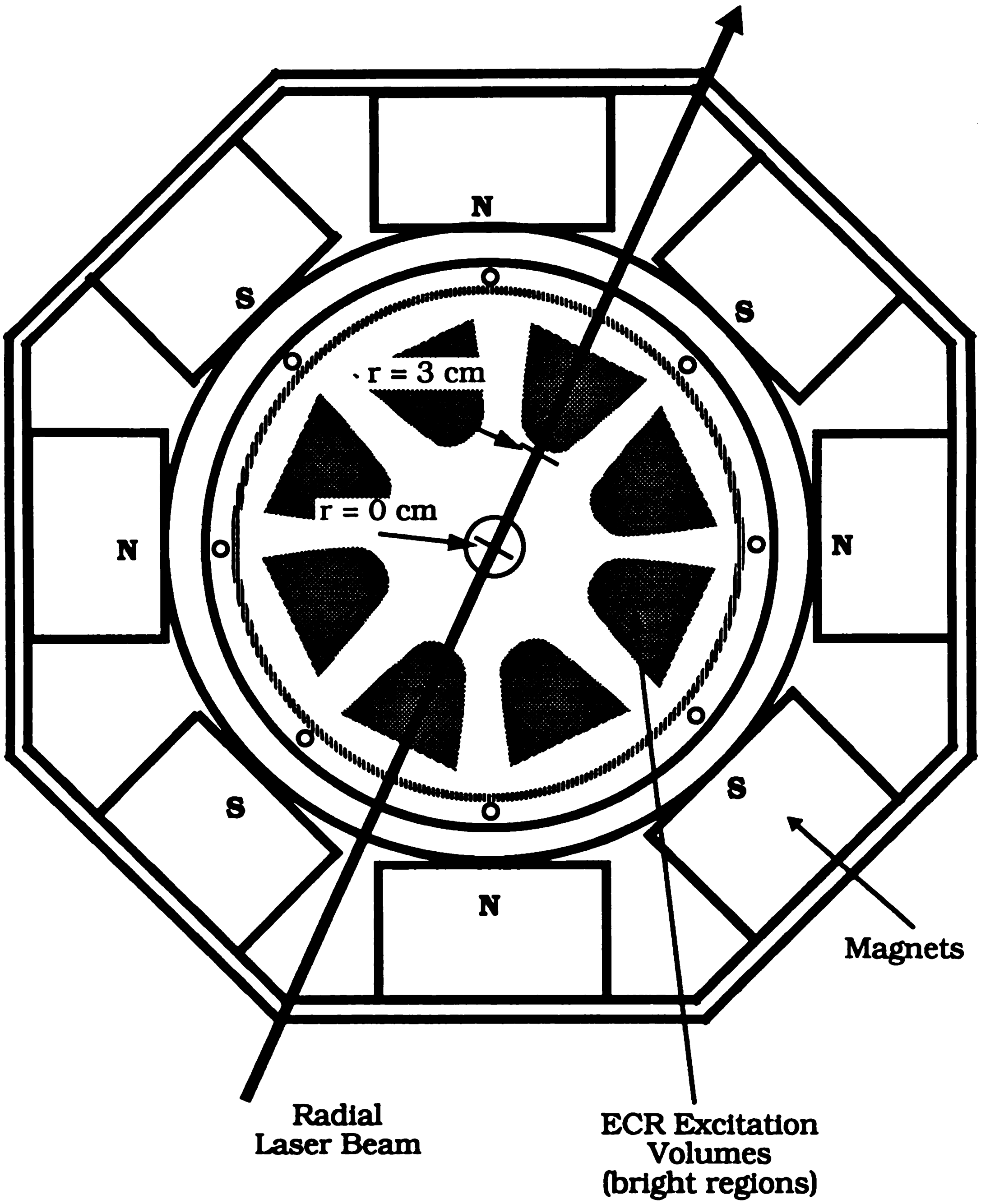

Figure 5.5: MPDR Baseplate - Top View Showing ECR Volumes

with increased gas flow (10 sccm to 40 sccm/0.43 mTorr to 1.31 mTorr) indicating the small affect that increased neutral density has on the number of ions in this gas flow/pressure range. With the applicability of the LIF system to ion density measurements verified, future experiments will characterize this reactor with respect to gas flow, pressure changes and microwave power to determine the operation of the MPDR reactor over a wider range of experimental conditions.

Chapter 6

Summary of Results

6.1 Implementation of an LIF System

A laser induced fluorescence system has been implemented for the characterization of an MPDR plasma. A pulsed Nd:YAG pumped dye laser is used to excite the plasma species. The subsequent fluoresced light is collected using a five centimeter focal length lens. The light, focused onto a one millimeter fiber cable, is filtered through a monochromator and measured with a photomultiplier. A gated integrator averages the fluoresced light intensity of each pulse. The resulting integrator signal is collected and averaged using a computer.

6.2 Testing of the LIF System

The application of the LIF system has been demonstrated for a number of measurements including ion energies, ion velocities and relative ion densities in an Argon plasma.

6.2.1 Ion Energy Measurements

Ion energy measurements are crucial to understanding ion bombardment during plasma processing. The LIF measurements quantify the energy of ions created in the ECR volumes of a microwave plasma disk reactor. Upper limit estimates of 0.5 eV ions give an understanding of these source energies for the MPDR plasma operating at a pressure of 0.75 mTorr with 240 Watts of microwave power and an argon gas flow of

20 sccm. The upper limit is necessary at this point since residual power and laser broadening may artificially affect the energy estimate.

6.2.2 Directed Ion Velocity Measurements

Plasma potential variation is one method that ions gain directed energy as they drift within the plasma. The velocity distribution shifts show an increase in directed energy (velocity) from the source to the processing region. These distributions are measured away from any magnetic fields and far from any surfaces; therefore, the measured shifts indicate a change in plasma potential of about 25 volts/meter over four centimeters from one centimeter to five centimeters below the magnets. This measurement was taken with 240 Watts of microwave power at a pressure of 0.75 mTorr with an argon gas flow of 20 sccm.

6.2.3 Relative Density Variation Measurements

The study of metastable species in this thesis gives insight into the density of ions within various regions of the plasma. An increase in microwave input power (150 W to 300 W) produces a corresponding increase in metastable ion density. These results match well with the total ion density measurements made using a double Langmuir probe.

A change in gas flow rate (10 sccm to 40 sccm/0.43 mTorr to 1.31 mTorr) produces no significant change in ion density over the range tested. The increase in neutral density associated with an increase in gas flow does not necessarily result in increased ionization.

An increase in chamber pressure (0.5 mTorr to 3 mTorr) with all other parameters held constant results in a decrease in metastable ion density above 1.5 mTorr. This measurement, taken at the center of the source, indicates a drop in excited species at the center.

6.3 Future Research

This thesis lays a foundation for future detailed studies of the MPDR ECR source using laser induced fluorescence. Using the techniques described here a complete study can be undertaken. Increased knowledge of the broadening mechanisms associated with energy measurements will refine the energy estimates. The ability to include a processing surface with bias to simulate the resulting plasma sheaths, the addition of downstream magnetic confinement and the use of other process gases will better simulate various processing conditions. Finally, extending the experimental parameter space through increased microwave power and an increased gas flow range will facilitate a complete characterization of the plasma.

APPENDIX

APPENDIX

QUICK BASIC PROGRAM FOR LIF SYSTEM CONTROL

The following program is used to control the gated integrator, the translation stages, the Nd:YAG laser and the grating angle within the dye laser. The code is written in Microsoft's QuickBasic version 4.0. The gated integrator is controlled through an HPIB interface. The Nd:YAG laser is controlled with a D/A convertor board (Metrabyte DAS-8). The grating angle is controlled through a stepper motor (Slo-Syn Model M061-LF-408E) and stepper motor controller (Slo-Syn Type 3180-PI125) connected through the serial port of the computer. The stages are controlled through a translation stage controller (Newport 860-c2) connected to the parallel port.

```
100     REM $INCLUDE: 'QB4SETUP'

        DIM INIT(15), POSI(3, 60), WAVARR(3, 60)
        DIM AVEOFF(15)
        DIM INARY%(7)
        DIM OUTARY%(7)

        BYTE% = 0 : MSTEP = 32
        GRATORD = 4: ISC& = 7: ADDR& = 728: MAX.LENGTH% = 20
        TIMEOUT.VAL! = 1!

              'Initialize serial port for control of stepper motor
        OPEN "COM1:9600,N,8,2,CS,DS,CD" FOR RANDOM AS #1

              'Set limit on forward and reverse operation of stepper motor
        PRINT #1, CHR$(17)
        PRINT #1, "<1 L18 +25000"
        PRINT #1, "<1 L19 -25000"
        PRINT #1, "<1 L41 0"

              'Initialize das8 data acquisition board
        MD% = 0
        BASADR% = &H300
        FLAG% = 0
        CALL DAS8(MD%, BASADR%, FLAG%)

        MD% = 14
        FLAG% = 0
        OP% = 9
        CALL DAS8(MD%, OP%, FLAG%)

        LOCATE , , 0
        PRINT "SET-UP"
        PRINT "  1) OP1 to Reed Relay"
        PRINT "  2) Reed Relay red and black to Laser Remote"
        PRINT "  3) Q-SW ADV SYNC to GI trigger"
        PRINT "  4) OP4 to RESET AVG on back of GI"

        PRINT

        PRINT "Enter filename to store data (.dat assumed) --"
        INPUT FILE1$
        FILE$ = "\boxcar\data\" + FILE1$ + ".dat"
        FILE2$ = "\boxcar\data\" + FILE1$ + "z.dat"
        FILE3$ = "\boxcar\data\" + FILE1$ + "y.dat"
        CLS
        GOSUB TIMEIT
        CLS
        OPEN FILE$ FOR OUTPUT AS #2
        OPEN FILE2$ FOR OUTPUT AS #3
        OPEN FILE3$ FOR OUTPUT AS #4

              'Initialize HPIB interface by: set-up address for GI
        CALL ioremote(ADDR&)
```

```
        IF PCIB.ERR <> NOERR THEN ERROR PCIB.BASERR
                    'Set value for length of time before timing out
        CALL iotimeout(isc&, timeout.val!)
        IF PCIB.ERR <> NOERR THEN ERROR PCIB.BASERR
                    'Clear channel
        CALL ioclear(isc&)
        IF PCIB.ERR <> NOERR THEN ERROR PCIB.BASERR

        R$ = ""
        S& = 0

MAIN:   WHILE (S& AND 1) = 0'                  Poll HPIB line for problems
             GOSUB SPOLL
        WEND
        PRINT                                  'Set up menu
        PRINT "ENTER CONDITION --"
        PRINT "    1 -- Laser on"
        PRINT "    2 -- Laser off"
        PRINT "    3 -- Automatic data collection"
        PRINT "    4 -- Manual wavelength adjustment (release motor torque)"
        PRINT "    5 -- User controlled motorized wavelength adjustment"
        PRINT "    q -- Quit data collection"

        R$ = INPUT$(1)
        PRINT
        N = 0

        A$ = "RDA" + CHR$(13)                  'set to read from channel A

        IF R$ = "1" THEN OP1% = 8: OP2% = 0'set data board to
                                               'turn on laser
        IF R$ = "2" THEN OP1% = 9: OP2% = 1'or turn off laser

        IF R$ = "1" OR R$ = "2" THEN
             GOSUB LASER
        PRINT
        PRINT TIME1, "MINUTE(S) TO GO"
        GOSUB RESETIT
        GOSUB WRITEA
        GOSUB READA
        INIT$ = B$
        FOR Z = 1 TO TIME
        NEXT Z
        GOSUB WRITEA
        GOSUB READA

        IF OP1% = 8 THEN OP1% = 9: OP2% = 1: GOSUB LASER
             DIFF& = VAL(B$) - VAL(INIT$)
             CLS
             PRINT DIFF&
        END IF

        IF R$ = "3" THEN
             CLS
```

```
                PRINT "ENTER CHOICE:"
                PRINT "     1 -- Increasing wavelength"
                PRINT "     2 -- Decreasing wavelength"
                PRINT "     3 -- Return to lower limit"
                PRINT "     4 -- Return to upper limit"
                PRINT "     5 -- Position scan (increasing only)"
                PRINT "     6 -- Single Averaged Data Point"
                PRINT "     e -- Back to Main Menu"
                PRINT
                S$ = INPUT$(1)

'If 1 is chosen the grating is changed after each data point to increase the wavelength
'of light. The length of the wavelength step is chosen by choosing the number of points
'taken per quarter angstrom of wavelength scan
                IF S$ = "1" OR S$ = "5" THEN
                        PRINT "Enter 15, 30, 45 or 60 ONLY"
REDO:                   INPUT "Enter number of data points PER quarter
                                angstrom --"; ND4%
                        IF (ND4% <> 15) AND (ND4% <> 30) AND
                        (ND4% <> 60) AND (ND4% <> 45) THEN GOTO REDO
                        INPUT "Enter lower laser n-number --"; N1
                        INPUT "Enter upper laser n-number --"; N2
                        L1 = N1 / gratord: L2 = N2 / gratord
                        ND% = ND4% * (N2 - N1): NPOS = 0
                        dir$ = "H07": WAVE = L1
                        IF ND4% = 60 THEN MSTEP = 8: DISP = .0042
                        IF ND4% = 45 THEN MSTEP = 12: DISP = .0063
                        IF ND4% = 30 THEN MSTEP = 16: DISP = .0083
                        IF ND4% = 15 THEN MSTEP = 32: DISP = .0167

                END IF

' Same as 1 except decreasing wavelength. Step should have already been set with 1.
                IF S$ = "2" THEN
                        INPUT "Enter lower laser n-number --"; N1
                        INPUT "Enter upper laser n-number --"; N2
                        L1 = N1 / gratord: L2 = N2 / gratord
                        ND% = 60 * (N2 - N1): NPOS = 0
                        dir$ = "H06": DISP = -.0042: WAVE = L2
                END IF

'3 and 4 return the grating angle to its original position after a scan
                IF S$ = "3" THEN
                        IF NPOS <> 0 THEN
                                FOR Y = 1 TO NPOS + 1
                                        PRINT #1, "<1"
                                        PRINT #1, "H06"
                                        FOR Z = 1 TO 25: NEXT Z
                                NEXT Y
                        ELSE
                                PRINT "Already at n ="; N1
                        END IF
                        GOTO DONE
                END IF
```

```
                IF S$ = "4" THEN
                        IF NPOS <> 0 THEN
                                FOR Y = 1 TO NPOS + 1
                                        PRINT #1, "<1"
                                        PRINT #1, "H07"
                                        FOR Z = 1 TO 25: NEXT Z
                                NEXT Y
                        ELSE
                                PRINT "Already at n ="; N2
                        END IF
                        GOTO DONE
                END IF

'If 6 is chosen from the main menu the data gathering is stopped to allow input of a
'particular pressure or power setting
                IF S$ = "6" THEN
BEGIN:                  INPUT "Enter Power or Pressure --"; PARAM
                        INITOT = 0
                        OP1% = 9: OP2% = 1
                        GOSUB LASER
                        PRINT #3, PARAM;
                        FOR Y = 1 TO 13
                                GOSUB RESETIT  'reset gi
                                GOSUB WRITEA   'send the command to read
                                        channel A (RDA)
                                 GOSUB READA   'read data from channel A
                                INIT$ = B$     'save the initial reading
                                FOR Z = 1 TO TIME: NEXT Z
                                GOSUB WRITEA
                                GOSUB READA    'write to gi and read in data
                                INIT(Y) = VAL(B$) - VAL(INIT$)
                                'data point is final-initial
                                'if Y is odd then laser was off and will be turned on
                                'else if Y is even then laser on and will be off
                                PRINT INIT(Y);
                                PRINT #3, INIT(Y);
                                IF (Y / 2!) <> INT(Y / 2!) THEN
                                        IF Y < 13 THEN     'if last this is last laser off
                                                OP1% = 8
                                                OP2% = 0
                                                GOSUB LASER
                                        END IF          'set DAS8 for Laser On
                                ELSE
                                        OP1% = 9        'set DAS8 for Laser Off
                                        OP2% = 1
                                        GOSUB LASER
                                END IF
                        NEXT Y
                        PRINT
                        AVEOFF(2) = (INIT(1) + INIT(3)) / 2    'average the laser off
                        AVEOFF(4) = (INIT(3) + INIT(5)) / 2    'values surrounding the
                        AVEOFF(6) = (INIT(5) + INIT(7)) / 2
                        AVEOFF(8) = (INIT(7) + INIT(9)) / 2
                        AVEOFF(10) = (INIT(9) + INIT(11)) / 2
```

```
                    AVEOFF(12) = (INIT(11) + INIT(13)) / 2    'laser on one
                    PRINT #3, " "

' each of the 3 intermediate data points is laser on minus average laser off
                    FOR Y = 2 TO 12 STEP 2
                         INITOT = INITOT + (INIT(Y) - AVEOFF(Y))
                    NEXT Y

' the ultimate data point is the average of the three intermediate ones
                    DIFF& = INITOT / 6

                    PRINT PARAM, DIFF&
                    PRINT #2, PARAM, DIFF&
                    IF INKEY$ <> "E" THEN
                         GOTO BEGIN
                    ELSE
                         S$ = "e"
                    END IF
               END IF
               IF S$ = "e" OR S$ = "E" THEN GOTO DONE

               TDIR% = 0

'Choosing  5 allows control of the z-axis of the translation stage.  Similar control of
'of the other two axes can be set up.
               IF S$ = "5" THEN
                    PRINT "SET z-axis TO TOPMOST POSITION"
                    PRINT
                    INPUT "Enter number of positions --"; PNUM
                    INPUT "Enter distance between positions (cm) --"; DIS
               END IF
               PRINT
               PRINT "NUMBER OF DATA POINTS:", ND%

 'Choosing 1, 2 or 5 brings the program here for the actual data collection
               FOR MOTOR = 1 TO ND%
                    q = 1
POSI:               M$ = ""
                    INITOT = 0
                    OP1% = 9: OP2% = 1
                    GOSUB LASER
                    PRINT #3, WAVE;
                    FOR Y = 1 TO 13
                              'Reset the gated integrator to 0
                         GOSUB RESETIT
                              'send the command to read channel A (RDA)
                         GOSUB WRITEA
                         GOSUB READA    'read data from channel A
                         INIT$ = B$     'save the initial reading
                         FOR Z = 1 TO TIME: NEXT Z
                         GOSUB WRITEA
                         GOSUB READA    'write to gi and read in data
                         INIT(Y) = VAL(B$) - VAL(INIT$)  'data point is final-initial
                              'if Y is odd then laser was off and will be turned on
```

```
            'else if Y is even then laser on and will be off
            PRINT #3, INIT(Y);
            IF (Y / 2!) <> INT(Y / 2!) THEN
                    IF Y < 13 THEN      'if last this is last laser off
                            OP1% = 8    'then don't set up for

                            OP2% = 0
                            GOSUB LASER
                     END IF             'set DAS8 for Laser On
            ELSE
                    OP1% = 9            'set DAS8 for Laser Off
                    OP2% = 1
                    GOSUB LASER
            END IF
    NEXT Y
    PRINT
    AVEOFF(2) = (INIT(1) + INIT(3)) / 2    'average the laser "off"
    AVEOFF(4) = (INIT(3) + INIT(5)) / 2    'values surrounding the
    AVEOFF(6) = (INIT(5) + INIT(7)) / 2    '  laser "on" values
    AVEOFF(8) = (INIT(7) + INIT(9)) / 2
    AVEOFF(10) = (INIT(9) + INIT(11)) / 2
    AVEOFF(12) = (INIT(11) + INIT(13)) / 2    'laser on one
    PRINT #3, " "

' each of the 3 intermediate data points is laser on minus average laser off
    FOR Y = 2 TO 12 STEP 2
            INITOT = INITOT + (INIT(Y) - AVEOFF(Y))
    NEXT Y

' the ultimate data point is the average of the three intermediate ones
    DIFF& = INITOT / 6

    PRINT WAVE, DIFF&, "Data point #"; MOTOR, NPOS
    POSI(q, MOTOR) = DIFF&
    WAVARR(q, MOTOR) = WAVE
    PRINT #2, WAVE, DIFF&
    IF S$ = "5" AND q < PNUM THEN
            GOSUB MOVE
            q = q + 1
            GOTO POSI
    END IF

    IF S$ = "5" AND q = PNUM THEN
            PRINT #2, " "
            TDIR% = NOT (TDIR%)
    END IF
    q = 1

    FOR Y = 1 TO MSTEP          'Move motor 8 "steps"
            PRINT #1, "<1"
            PRINT #1, dir$
            FOR Z = 1 TO 25: NEXT Z
    NEXT Y
    NPOS = NPOS + MSTEP
```

```
                        WAVE = WAVE + DISP
                        IF INKEY$ = "E" OR M$ = "E" THEN MOTOR = ND%
80                  NEXT MOTOR
        END IF

        FOR Y = 1 TO 3
                FOR Z = 1 TO ND%
                        PRINT #4, WAVARR(Y, Z), POSI(Y, Z)
                NEXT Z
                PRINT #4, " "
        NEXT Y

        IF R$ = "4" THEN GOSUB MANUAL
        IF R$ = "5" THEN GOSUB MOTCON
        IF R$ = "q" OR R$ = "Q" THEN GOSUB DATEND
DONE:   GOTO MAIN

        ------------------------------------------------------------
                        BEGIN SUBROUTINES
        ------------------------------------------------------------

'This subroutine puts the command A$ on the HPIB line for the Gated Integrator
WRITEA:         LENGTH% = LEN(A$)
                CALL iooutputs(ADDR&, A$, LENGTH%)
                IF PCIB.ERR <> NOERR THEN ERROR PCIB.BASERR
                RETURN

'This subroutine reads the HPIB line to get the data B$ from the Gate Integrator
READA:          B$ = SPACE$(20)
                S& = 0
                WHILE (S& AND 1) = 0
                        GOSUB SPOLL
                        IF (S& AND 128) THEN
                        CALL ioenters(ADDR&, B$, MAX.LENGTH%, ACTUAL.LENGTH%)
                        IF PCIB.ERR <> NOERR THEN ERROR PCIB.BASERR
                        END IF
                WEND
                RETURN

'This subroutine polls the HPIB line for errors or busy signals
SPOLL:          CALL iospoll(ADDR&, S&)
                IF PCIB.ERR <> NOERR THEN ERROR PCIB.BASERR
                RETURN


'This subroutine sends  the command  to release motor torque to the stepper motor
MANUAL:         CLS
                INPUT "Are you sure you want to LOSE motor position"; M$
                IF M$ = "y" OR M$ = "Y" THEN
                        PRINT #1, "<1 N000 G68"
                        FOR Z = 1 TO 25: NEXT Z
                        PRINT #1, "<1 H01"
                        FOR Z = 1 TO 2: NEXT Z
                        CLS
```

```
                PRINT "Press any key to lock motor and continue..."
                DO WHILE INKEY$ = "": LOOP
                PRINT #1, "<1 N000 G69"
                FOR Z = 1 TO 25: NEXT Z
                PRINT #1, "<1 H01"
                FOR Z = 1 TO 25: NEXT Z
                PRINT #1, "<1 H09"
                FOR Z = 1 TO 25: NEXT Z
        END IF
        RETURN
```

This subroutine allows step by step movement of the grating angle. The length of 'each step depends on the number of data points chosen for the interval measured

```
MOTCON: CLS
        INPUT "Are you sure you want to LOSE motor position"; M$
CONT:   IF M$ = "y" OR M$ = "Y" THEN
                PRINT "Increase, Decrease or End (i, d or e)"
                M$ = INPUT$(1)
                IF M$ = "i" OR M$ = "I" THEN
                        FOR Y = 1 TO MSTEP
                                PRINT #1, "<1 H07"
                                FOR Z = 1 TO 25: NEXT Z
                        NEXT Y
                END IF

                IF M$ = "d" OR M$ = "D" THEN
                        FOR Y = 1 TO MSTEP
                                PRINT #1, "<1 H06"
                                FOR Z = 1 TO 25: NEXT Z
                        NEXT Y
                END IF

                IF M$ = "e" OR M$ = "E" THEN
                        RETURN
                ELSE
                        M$ = "Y"
                        GOTO CONT
                END IF
        END IF
        RETURN
```

This subroutine either turns on the laser beam or turns it off depending on OP1%

```
LASER:  MD% = 14
        FLAG% = 0
        OP% = OP1%
        CALL DAS8(MD%, OP%, FLAG%)
        FOR Z = 1 TO 4000: NEXT Z
        RETURN
```

This subroutine prints the current data file to the screen for a quick scan

```
SHOW:   CLS
        CLOSE #2
        OPEN FILE$ FOR INPUT AS #2
```

```
                WHILE NOT EOF(2)
                        INPUT #2, WAVE, DIFF&
                        PRINT WAVE, DIFF&
                WEND
                PRINT
                CLOSE #2
                OPEN FILE$ FOR APPEND AS #2
                RETURN

'This is a menu of options shown when "q" is chosen from the main menu
DATEND:         CLS
                PRINT "Enter 1 -- To Show Data"
                PRINT "       2 -- Resume Data Collection"
                PRINT "       3 -- Change sample time"
                PRINT "       4 -- Change grating order"
                PRINT "       e -- Exit program"
                R$ = INPUT$(1)

                IF R$ = "e" OR R$ = "E" THEN GOTO QUIT

                IF R$ = "1" THEN GOSUB SHOW
                IF R$ = "2" THEN PRINT
                F R$ = "3" THEN GOSUB TIMEIT
                IF R$ = "4" THEN GOSUB GRATE
                RETURN

'This computes the loop timing from the minutes entered by the user
TIMEIT:         INPUT "Enter sample time in minutes--"; TIME1
                CLS
                TIME = TIME1 * 413000
                PULSES = TIME1 * 600  'TIME1 * 60 sec * 10 pulses/sec
                RETURN

'This allows changing the grating order for data point calculations
GRATE:          CLS
                INPUT "Enter new grating order --"; gratord
                RETURN

'This routine moves the translation stages the specified number of cm
MOVE:           IF ((BYTE% AND &H2) = 0) THEN
                        CALL INT86OLD(&H17, INARY%(), OUTARY%())
                        BYTE% = BYTE% OR &H60
                        CALL INT86OLD(&H17, INARY%(), OUTARY%())
                        IF (((BYTE% AND &H2) = 0) AND ((BYTE% AND &H8) = 0)) THEN
                                BYTE% = BYTE% AND &HDF
                                CALL INT86OLD(&H17, INARY%(), OUTARY%())
                        END IF
                END IF

                IF TDIR% = -1 THEN                      'move z-axis forward
                        BYTE% = BYTE% OR &H23
                        INARY%(0) = BYTE%
                        INARY%(3) = 0
```

```
                'velocity of z-axis motor (cm/sec) at maximum dial setting in rev
                ZZ = 16.1
                CALL INT86OLD(&H17, INARY%(), OUTARY%())
                GOSUB TMOVE
                INARY%(0) = BYTE% AND &HFD
                CALL INT86OLD(&H17, INARY%(), OUTARY%())

        ELSEIF TDIR% = 0 THEN               'move z in reverse
                BYTE% = (BYTE% AND &HFE) OR &H22
                INARY%(0) = BYTE%
                INARY%(3) = 0
                'velocity of z-axis motor (cm/sec) at maximum dial setting in rev
                ZZ = 16.3
                CALL INT86OLD(&H17, INARY%(), OUTARY%())
                GOSUB TMOVE
                INARY%(0) = BYTE% AND &HFD
                CALL INT86OLD(&H17, INARY%(), OUTARY%())
        END IF
        RETURN

'This subroutine times the movement of the stage for a know stage velocity (zz)
TMOVE:  START = TIMER
        STOPIT = START + ZZ * DIS
        WHILE (STOPIT > TIMER)
        WEND
        RETURN

'This routine resets the gated integrator by sending a pulse to the RESET AVE input
RESETIT:        MD% = 14
        OP% = OP2%
        CALL DAS8(MD%, OP%, FLAG%)
        FOR X = 1 TO 350: NEXT X
        OP% = OP1%
        CALL DAS8(MD%, OP%, FLAG%)
        FOR X = 1 TO 3000:NEXT X
        RETURN

QUIT:   CLOSE
        END
```

LIST OF REFERENCES

LIST OF REFERENCES

[1] J. Asmussen," Electron Cyclotron Resonance Microwave Discharges for Etching and Thin-film Deposition," J. Vac. Sci. Technol., A 7, 3, (1989)

[2] J. Hopwood, M. Dahimene, D. K. Reinhard, J. Asmussen, "Plasma Etching with a Microwave Cavity Plasma Disk Source," J. Vac. Sci. Technol., B 6, 1, (1988).

[3] T. Roppel, D. K. Reinhard, J. Asmussen, "Low Temperature Oxidation of Silicon Using a Microwave Plasma Disk Source," J. Vac. Sci., Technol., B 4, 1 (1986).

[4] J. Hopwood, D. K. Reinhard, J. Asmussen, "Charged Particle Densities and Energy Distributions in a Multipolar Electron Cyclotron Resonant Plasma Etching Source," J. Vac. Sci. Technol., A 8, 4, (1990).

[5] L. D. Radziemski, editor, Laser Spectroscopy and its Applications, (Marcel, Dekker, New York, 1987).

[6] J. W. Daily, "Saturation Effects in Laser Induced Fluorescence Spectroscopy," Applied Optics, Vol. 16, No. 3, (1977).

[7] D. J. Trevor, N. Sadeghi, T. Nakano, J. Derouard, R. A. Gottscho, P. D. Foo, J. M. Cook, "Spatially Resolved Ion Velocity Distributions in a Diverging Field Electron Cyclotron Resonance Plasma Reactor," Appl. Phys. Lett., 57, 12, (1990).

[8] R. B. Wright, C. E. Young, M. J. Pellin, D. M. Gruen, "High Resolution COntinuous Wave Laser Induced Fluorescence Spectroscopy of Sputtered Zr Atoms," J. Vac. Sci. Technol., 20, 3, (1982).

[9] H. R. Griem, Plasma Spectroscopy, (McGraw Hill, New York, 1964).

[10] A. C. Eckbreth, P. A. Bonczyk, J. F. Verdieck, "Combustion Diagnostics by Laser Raman and Fluorescence Techniques," Prog. Energy Combust. Sci., Vol. 5, (1979).

[11] R. B. Wright, M. J. Pellin, D. M. Gruen, "Velocity Distribution of Sputtered Zr Atoms as Determined by Laser Induced Fluorescence Spectroscopy," Surface Science, 110, (1981).

[12] N. Sadeghi, T. Nakano, D. Trevor, R. A. Gottscho, "Ion Transport in an Electron Cyclotron Resonance Plasma", to be published J. Appl. Phys.

[13] T. Nakano, N. Sadeghi, R. A. Gottscho, "Ion and Neutral Temperatures in Electron Cyclotron Resonance Plasma Reactors", Appl. Phys. Lett., 58, 5, (1991).

[14] E. A. Den Hartog, H. Persing, R. C. Woods, "Laser Induced Fluorescence Measurements of Transverse Ion Temperature in an Electron Cyclotron Resonance Plasma", Appl. Phys. Lett., 57, (1990).

[15] S. D. Rosner, T. D. Gaily, R. A. Holt, "Laser Fluorescence Measurement of Relative Electron Impact Cross Sections for Metastable States of Ar^+ and Xe+,"" J. Phys. B: Atom. Molec. Phys., Vol. 9, No. 16, (1976).

[16] Y. Watanabe, M. Shiratam, S. Ogi, N. Kunihiro, "Study on Electron Density Dependence of Metastable Ar+ Density in Pulsed-discharge Plasma by Using LIF Method," Jap. J. Appl. Phys., Vol. 26, No. 1, (1987).

[17] S. G. Hansen, G. Luckman, G. C. Nieman, S. D. Colson, "Formation and Decay of Metastable Fluorine Atoms in Pulsed Fluorocarbon/Oxygen Discharges Monitored by Laser Induced Fluorescence," Appl. Phys. Lett., 56, 8, (1990).

[18] K. Ninomiya, K. Suzuki, S. Nishimatsu, O. Okada, "Diagnostics of Microwave Plasma by Laser Induced Fluorescence," J. Vac. Sci. Technol., A 4, 3, (1986).

[19] M. Heaven, T. A. Miller, R. R. Freeman, J. C. White, J. Bokor, "Two-Photon Absorption, Laser Induced Fluorescence Detection of Cl Atoms," Chem. Phy. Lett., Vol 86, No. 5-6, (1982).

[20] G. S. Selwyn, L. D. Baston, H. H. Sawin, "Detection of Cl and Chlorine-containing Negative Ions in RF Plasmas by Two-Photon Laser Induced Fluorescence," Appl. Phys. Lett., 51, 12, (1987).

[21] N. Hata, A. Matsuda, K. Tanaka, "Spectroscopic Diagnostics of Plasma-Chemical-Vapor Deposition from Silane and Germane," J. Appl. Phys., 61, 8, (1987).

[22] B. L. Preppernau, D. A. Dolson, R. A. Gottscho, T. A. Miller, "Temporally Resolved Laser Diagnostic Measurements of Atomic Hydrogen Concentrations in RF Plasma Discharges," Plasma Chemistry and Plasma Processing, Vol. 9, No. 2, (1989).

[23] G. S. Selwyn, "Spatially Resolved Detection of O Atoms in Etching Plasmas by Two-Photon Laser Induced Fluorescence," J. Appl. Phys., 60, 8, (1986).

[24] L. F. Dimauro, R. A. Gottscho, T. A. Miller, "Two-Photon Laser Induced Fluorescence Monitoring of O Atoms in a Plasma Etching Environment," J. Appl. Phys., 56, 7, (1984).

[25] K. E. Greenberg, P. J. Hargis, Jr., "Laser Induced Fluorescence Detection of SO and SO_2 in SF_6/O_2 Plasma Etching Discharges," J. Appl. Phys., 68, 2, (1990).

[26] J. A. Hopwood, Macroscopic Properties of a Multipolar Electron Cyclotron Resonance Microwave-cavity Plasma Source for Anisotropic Silicon Etching, Ph.D. Dissertation, Michigan State University, 1990.

[27] P. Mak, G. King, J. Hopwood, T. Grotjohn, J. Asmussen, "Influence of Static Magnetic Field Configuration and EM Field Pattern on ECR Discharge Performance", presented: IEEE International Conference on Plasma Science, 1991.

[28] P. Horwitz, W. Hill, The Art of Electronics, (Cambridge University Press, Cambridge, 1988), p. 587.

[29] J. Hopwood, D. K. Reinhard, J. Asmussen, "Experimental Conditions for Uniform Anisotropic Etching of silicon with a microwave Electron Cyclotron Resonance Plasma System," J. Vac. Sci. Technol., B 6, 6, (1988).

[30] M. Dahimene, Development of a Microwave Ion and Plasma Source Immersed in a Multicusp Electron Cyclotron Resonant Magnetic Field, Ph. D. Dissertation, Michigan State University, (1987).

[31] T. A. Miller, "Optical Emission and Laser Induced Fluorescence Diagnostics in Reactive Plasmas," J. Vac. Sci. Technol., A 4, 3, (1886).

[32] T. A. Miller, "Novel Techniques for Plasma Diagnostics: Electron Paramagnetic Resonance and Laser Induced Fluorescence Spectroscopy," Plasma Chemistry and Plasma Processing, Vol. 1, No. 1, (1981).

[33] S. M. Rossnagel, J. J. Cuomo, W. D. Westwood, eds., Handbook of Plasma Processing Technology, (Noyes, New Jersey, 1990).

[34] Y. Arata, S. Miyake, H. Matsuoka, "Laser Induced Fluorescence and Doppler Free Polarization Spectra in a Low Density Hydrogen Plasma," Jap. J. Appl. Phys., Vol. 26, No. 3, (1987).

[35] D. M. Manos, D. L. Flamm, eds., Plasma Etching: An Introduction, (Academic Press, San Diego, 1989).

[36] M. Venugopalan, "Aim a Laser at Your Plasma and Expose Its Secrets," Research and Development, June 1989.

[37] J. N. Ross, "Perturbation Spectroscopy of an Argon Laser Discharge Using a Tunable Dye Laser," J. Phys. B, Vol. 8, No. 4, (1975).

[38] K. Ninomiya, K. Suzuki, S. Nishimatsu, O. Okada, "Diagnostics of Microwave Plasma by Laser Induced Fluorescence," J. Vac. Sci, Technol., A 4, 3, (1986).